NOVA SCHOOL OF SCIENCE & TECHNOLOGY

DEPARTMENT OF MATERIALS ENGINEERING

**ALBERTO CARLOS VERDES VALE REGO**

# RECYCLING OF WASTEPAPER INTO FUNCTIONALIZED ELECTRONIC PAPER

"Sustainability is here to stay, or we may not be" – Niall Fitzgerald

MASTER IN MATERIAL ENGINEERING

NOVA University Lisbon

November 2021

NOVA SCHOOL OF SCIENCE & TECHNOLOGY

DEPARTMENT OF MATERIALS ENGINEERING

# RECYCLING OF WATEPAPER INTO FUNCTIONALIZED ELECTRONIC PAPER

"Sustainability is here to stay, or we may not be" – Niall Fitzgerald

**ALBERTO CARLOS VERDES VALE REGO**

Integrated Master in Materials Engineering

**Adviser:** Dr. Suman Nandy
*Researcher Investigator, CENIMAT-i3N*

**Co-advisers:** Dr. Diana Gaspar
Researcher, Alma Science

**Examination Committee:**

**Chair:** Dr. Alexandre Velhinho,
Auxiliar Professor, DCM|FCT-NOVA

**Rapporteurs:** Dr. Jonas Deuermeier,
PhD Investigator, DCM|FCT-NOVA

**Members:** Suman Nandy,
Researcher Investigator, CENIMAT-i3N

MASTER IN MATERIALS ENGINEERING

NOVA University Lisbon
November 2021

**RECYCLING OF WASTEPAPER INTO FUNCTIONALIZED ELECTRONIC PAPER**

Dedico este trabalho a toda a minha família e amigos.

# Acknowledgments

This thesis is the culmination of all the hard work accomplished in the last years, which fortunately were done with extraordinary support. An academic year in which one of the biggest pandemics ever occurred, where barriers were created which thankfully were overcome.

Firstly, I want to thank the faculty, FCT-UNL, for the availability of all the materials, chemicals, and instruments of characterization available in the laboratories, to all my supervisors for all the commitment and flexibility throughout this year, where they made this work much easier and more accessible, and a special appreciation to the directors of the Materials Research Center, Prof. Elvira Fortunato (CENIMAT) and Prof. Rodrigo Martins (CEMOP). Thanks to Suman Nandy for the energy, devotion, and enthusiasm to implement all their knowledge for the execution of this work. To Professor Diana Gaspar for all the devotion to this project that was embraced with such affection.

Sincerely appreciate Guilherme Ferreira, Ph.D. student, that helped and support the achievement of this project, he was ALWAYS available to follow all phases of it, and with an exceptional willingness to solve new challenges put into practice. To Sumita Goswami for her assistance in several critical moments.

I want to thank all my friends, college, and work colleagues, for all the follow-ups.

My deepest gratitude goes to my entire family: my parents, grandparents, and sister for all the guidance and effort gained throughout these academic years. To Raquel, for being the one who was most present at this moment of my life.

# Abstract

One of the main objectives of this work has in view a concern of our society: Sustainability. With the degradation of the planet's well-being and environmental quality, and being an increasingly irreversible process in recent years, it only makes sense to focus all our attention on improving sustainability and reducing electronic waste, following the vision of UN Sustainable Goals and the European Green Deal.

This work is committed to the fabrication of multi-functional electronic paper (e-paper) through recycling the waste in a low-cost method, targeted to reduce the use of critical raw materials. Furthermore, the e-paper has been designed for multi-purpose smart applications such as mechano-responsive energy harvesters, interactive pressure sensors, or energy storage systems. This work is based on studies previously carried out at CENIMAT and CEMOP. However, this work aims at a more ecological approach, as it uses cellulose obtained from used newspapers that would have no other destination than recycling.

All recycled samples and fabricated electronic devices were investigated by using chemical, electrical, and morphological characterization techniques. The successful functionalization of recycled paper (RP) showed good performance as an e-paper.

The e-paper has been designed for a mechano-responsive energy harvesting device, that generates current under charge transfer mechanism at PANI-Cellulose/electrode Interface layer. The manufactured devices present satisfactory results (output voltage: 17 - 20 V, output current: 0.85 - 1.6 μA, power density: 0.16 - 0.35 $Wm^{-2}$) in the production of energy through mechanical impulses, managing to light up several LEDs in series.

Moreover, the E-paper has been investigated as a flexible paper-based pressure sensor. The device demonstrates excellent sensitivity, fast response, and a wide working range from 10 Pa to 10 kPa.

Keywords: Eco-design, e-Waste, Cellulose, Polyaniline, Electronic Paper, Energy Harvester Sensor

# Resumo

Um dos principais objetivos deste trabalho tem em vista uma preocupação da nossa sociedade: Sustentabilidade. Com a degradação do bem-estar e qualidade ambiental do planeta, e sendo um processo cada vez mais irreversível nos últimos anos, só faz sentido concentrar toda a nossa atenção na melhoria da sustentabilidade e na redução do lixo eletrônico, seguindo a visão dos Objetivos de Sustentabilidade das Nações Unidas e do Acordo Verde Europeu.

Este trabalho está comprometido com a fabricação de papel eletrónico multifuncional de baixo custo através de lixo reciclado, visado em reduzir o uso de matérias-primas em estado critico. De seguida, o papel eletrónico foi projetado em diversas aplicações de multiuso inteligente como extração de energia através de resposta mecânica, sensores de pressão interativos e sistemas de armazenamento de energia. Este trabalho tem por base estudos anteriormente desenvolvidos no CENIMAT e CEMOP. No entanto, este trabalho visa uma abordagem mais ecológica, pois utiliza celulose obtida de jornais usados que não teriam outro destino senão a reciclagem.

Todas as amostras recicladas e papel eletrónico foram investigadas através de caracterizações químicas, elétricas e morfológicas. Ao funcionalizar o papel reciclável (RP), este demonstrou boa condutividade como papel eletrónico.

O papel eletrónico foi projetado em dispositivos de extração de energia através de resposta mecânica que por sua vez, geraram corrente com um mecanismo de transferência de carga num sistema PANI-celulose/elétrodo. Os dispositivos fabricados, apresentaram resultados satisfatórios (tensão de saída: 17-20 V, corrente de saída: 0.85 -1.6 μA, densidade de potência: 0.16-0.35 $Wm^{-2}$) na produção de energia através de impulsos mecânicos, conseguindo acender vários LEDs em série.

Posteriormente, o papel eletrónico foi investigado como sensor de pressão flexível. O dispositivo demonstrou excelente sensibilidade, resposta rápida e uma larga área de trabalho entre 10 Pa e 10 kPa.

Palavras-chave: Design Ecológico, Lixo Eletrónico, Celulose, Polianilina, Papel Eletrônico, Sensores de Transferência de Energia.

# Contents


1 INTRODUCTION ..... 1

1.1 Eco-design Strategies ..... 2

1.2 Paper in Electronics ..... 2

1.3 Polyaniline as Electronic Material ..... 3

1.4 Electronic Paper for Smart Applications ..... 4

1.4.1 Mechano-responsive Energy Harvester ..... 4

1.4.2 Pressure Sensors ..... 5

2 MATERIALS AND METHODS ..... 8

2.1 Reagents ..... 8

2.2 Recycling of the Newspaper ..... 8

2.3 Fabrication of Recycled Cellulose-PANI Electronic Devices ..... 9

2.3.1 Recycled Paper Fabrication ..... 9

2.3.2 Functionalization of Recycled Paper ..... 9

2.3.3 Fabrication of Electrodes ..... 10

2.3.4 Fabrication of the Eco-smart Devices: Energy Harvester and Pressure Sensors ..... 10

2.4 Characterization Techniques ..... 12

2.4.1 Morphological, Chemical, and Compositional Characterization ..... 12

2.4.2 Optical Characterization ..... 12

2.4.3 Electrical Characterization ..... 12

3 RESULTS AND DISCUSSION ..... 14

3.1 Recycling of the Newspaper ..... 14

3.2 Samples Fabrication ..... 15

3.2.1 Selectivity and Processing ..... 15

3.2.2 Measurements and Morphological Analysis ..... 16

3.3 Cellulose Samples Polymerization ..... 19

3.3.1 Chemical and Morphological Analyses ..... 19

3.3.2 Electrical analysis ..... 23
3.4 Functionalized Energy Devices ..... 25
3.4.1 Electrical Analyses ..... 26
3.4.2 Eco-Energy Devices Applications ..... 29
3.5 Pressure Sensors ..... 29
4 CONCLUSIONS AND FUTURE PERSPECTIVES ..... 34
REFERENCES ..... 38
ANNEXES ..... 45

# List of Tables

**Table 3.1** - Reagents quantity on all samples. ..... 17
**Table 3.2** - Recycled paper (RP) samples characteristics. ..... 17
**Table 3.3** - Electrical properties of all samples surface measured with a Hall Effect System (HES). . 25
**Table 3.4** - Average output voltage on open circuit ($V_{oc}$) and output current with a 100M ohm load resistance on a short circuit ($I_{sc}$); (energy harvesting with mechanic stimuli)..... 26

# List of Figures

**Figure 1.1** - Paper life-cycle from the raw material to the ecological energy devices (thesis work). .... 2
**Figure 1.2** - Paper recycling integration on Circular Economy. .... 3
**Figure 1.3** - Mechano-responsive charge transfer on PANI recycled cellulose. .... 5
**Figure 2.1** - Functionalization via suspension (deep-cast method). 1– Solution A and B with respective chemicals; 2- Solution A mixed on solution B in a 1:2 ratio; 3-Synthesized Polyaniline (emeraldine): dark greenish-blue; 4- immersion of the samples on the solution (2 minutes); 5- RFP sample functionalized after dried at room temperature. .... 10
**Figure 2.2** - Illustration of the layers montage on the eco-smart devices for energy harvesting: Two charge collector layers (CCL) of silver and one active layer (AL) which is the functionalized cellulose sample. Both layers were encapsulated with commercial tape and two copper tapes were connected on the sides to prevent damage to the CCL. .... 11
**Figure 2.3** - Illustration of the layers montage on the eco-smart devices for resistive pressure sensors: One charge collector layer (CCL) of silver and one active layer (AL) screen printed on one surface with silver ink. Both layers were encapsulated with white paper and commercial tape. .... 11
**Figure 3.1** - Newspaper and fibers obtained during the recycling process. .... 15
**Figure 3.2** - SEM morphological analysis of the RP samples cross-section (1mm) images. Images a), b), c) and d) correspond to samples RP1, RP2, RP3 and RP4, respectively. .... 18
**Figure 3.3** - A comparison of both functionalization methods via SEM (scale of 300 μM) and a photograph of each sample. a) two-step drop-cast method; b) suspension/deep-cast method. On a) the functionalization was not achieved as seen by the absence of PANI on the fibers and the yellow color of the samples, on the contrary b) presents a dark greenish-blue color which confirms the presence of emeraldine salt. .... 20
**Figure 3.4** - SEM Image of all functionalized samples with PANI with suspension/deep-cast method. a) RFP1; b) RFP2; c) RFP3; d) RFP4. In the inset is presented a photograph of each sample. .... 21
**Figure 3.5** - Comparison of ATR-FTIR spectra curves before and after functionalization of each sample; Spectra for pristine and PANI functionalized samples: a) RP1 and RFP1 spectra with the PANI bands with correspondent designation (same on the other graphs); b) RP2 RFP2; c) RP3 and RFP3; d) RP4 and RFP4. The dashed lines are related to the characteristic PANI absorption bands present for every RFP sample spectrum. .... 23
**Figure 3.6** - Biorad HL5500 Hall Effect System (HES) and an example of a sample setup with the four-probe pointers fixed on each edge of its. .... 24
**Figure 3.7** - Plots of output mechano-responsive current and output voltage of all RFP devices. a) presents the average peaks of output voltage on an open circuit of all devices and b) presents the average output current on a short circuit of all devices. .... 27
**Figure 3.8** - Current density and power density for different load resistances applied in series to the device. These results were achieved due to output voltage from mechano-responsive stimulus on each RFP energy devices. .... 28

**Figure 3.9** - Photograph of device RFP3 electrical output performance on flash lighting 6 LEDs connected in series and respective schematic of the rectifier circuit. ..... 29
**Figure 3.10** - Schematic representation of the paper-based pressure sensors (unloading and loading mechanism). ..... 30
**Figure 3.11** - a) Pressure sensor circuit; b) Up-close photograph of the pressure sensor with 8g weights; c) photo of the pressure sensor overall output characterization with an Arduino board and a 100 kΩ load resistance. ..... 31
**Figure 3.12** - Electrical characterization of the pressure sensor: RFP3. a) Voltage monitored over time for five loading weights (measuring time: 120 seconds); b) Electrical performance of the device when submitted to several loading/unloading cycles. The protocol followed was: 15 seconds loaded, and 15 seconds recovery. ..... 32
**Figure A.1** - Polyaniline synthesis for the deep-casting functionalization, the dark greenish-blue color confirms the emeraldine salt oxidation.....44
**Figure A.2** - Photograph of the silver ink electrode used as charge collector on the energy devices....44
**Figure B.1 –** Step-by-step photographs of the newspaper recycling process.....45
**Figure B.2 -** Final recycled paper (RP) samples before functionalization.....45
**Figure B.3 -** Step-by-step photographs of the deep-cast method (suspension) of RP.....46
**Figure B.4 -** Sample functionalized with two-step drop-casting method (left) and sample functionalized with suspension/deep-casting method (right). Emeraldine state was achieved on the suspension method (dark greenish-blue) and not achieved on the drop-casting method (greenish-yellow).....46
**Figure B.5** – Open circuit ($V_{oc}$) and short circuit ($I_{sc}$) rectifier, respectively.....47

# List of abbreviations

AL - Active Layer
APS – Ammonium Persulfate
ATR - Attenuated Total Reflectance
ATR-FTIR – Fourier-transform infrared spectroscopy with attenuated total reflectance
BW – Black and White
CA – Citric Acid
CCL - Charge Collector Layer
CE - Circular Economy
CEMOP – Centre of Excellence in Microelectronics Optoelectronics and Processes
CENIMAT – Centro de investigação de Materiais.
CSA - Camphor-10-Sulfonic Acid
e-waste - Electronic Waste
EDS - Energy-Dispersion Spectroscopy
EU – European Union
FTIR - Fourier-transform Infrared
GPS – Global Positioning System
HES - Hall Effect System
LED - Light Emitting Diode
P-TENG - Paper Triboelectric Nanogenerator.
PANI – Polyaniline
PCA - Polycarboxylic Acid
PS - Polystyrene
RFP - Recycled Functionalized Paper
RP - Recycled Paper
Rsh – Sheet resistance
SC - Supercapacitor
SDS - Sodium Dodecyl Sulfate
SEM - Scanning Electron Microscopy
UN – United Nation
W/W – Weight per Weight

# List of symbols

I – Current

P – Power

R – Resistance

$R_{sh}$ – Sheet Resistance

$I_{sc}$ – Short circuit output current

$V_{oc}$ – Open circuit output voltage

$I_{max}$ – Maximum current density

$P_{max}$ – Maximum power density

# Motivation and objectives

We are living in a digital era, where electronics are indispensable for most people around the world. With the increase of the use of electronics consumables, the amount of electronic waste (e-waste), resulted after the product expiry, is increasing simultaneously [1]. The increment of e-waste is a real problem for our environment, as most of the e-wastes are hard to recycle and dispose in an eco-friendly manner. It is vital to seek for solutions to prevent our planet to collapse from it.

To find a viable and safe way of minimizing toxic e-waste and excess use of critical raw materials from electronic devices, one of the challenges is to find alternatives by developing product eco-design strategies and step to a circular economy. In this context, paper or cellulose substrate has a great impact as promising materials towards the shift of ecological alternatives. This thesis is focused on these changes, to make ecological progress that will adjust our environmental footprint in the future.

The present work is fully committed to finding viable options to replace some of the materials commonly used in electronic devices, most of them expensive or unsustainable, by paper due to its recycling properties and availability. In this work, it was targeted the development of cellulose-based matrices and their functionalization with conductive polymer to produce devices capable of harvesting energy of the electric energy generated by a mechanical stimulus. With this process, the aim was to fabricate an eco-designed energy harvester.

Having in mind the ecological impact, the cellulose matrices were produced from recycled newspapers, using several reagents to reach desired properties of the cellulose, such as flexibility and sponginess, to be furtherly functionalized with Polyaniline (PANI). The bonding of a conjugated polymer with cellulose results in cellulose-based matrices with higher conductive properties, which together with electrode layers of silver ink will work as an energy harvesting device, producing piezoelectric energy with human motion. In this manner, the way that the PANI reacts with the cellulose substrate, and the different reagents were studied together along with the full characterization of the developed energy device.

Furtherly, the success of the charge transfer mechanism of the devices motivated this work to the next step leading to the production of resistive paper-based pressure sensors.

# 1 INTRODUCTION

The impact of electronic waste or e-waste on planet Earth is increasing exponentially, demanding the establishment of ecological measures to prevent the decline of the world environment. With the consumption increase of electronic devices along the century, the amount of e-waste is growing fast mostly in high-developed countries. Most of these e-wastes are transported to developing countries from developed countries. Due to the lack of effective legislation, this e-waste is regulated for recycling in a poor condition and unsecured way [2]. According to the UN´s Global E-waste Monitor, most of the e-waste is not systematically collected or recycled. Due to the demand of low-priced electronics, the e-wastes are sometimes reused in a new products without proper treatment and reprocessing. This leads to unhealthy systems in the consumer's market.

In 2016, only 20% of e-waste was recycled globally and from the 44.7 million metric tons (estimated 6.5 kg per capita) of e-waste generated, an estimated 55 billion euros of valuable resources[1] were wasted [3]. In the year 2019 53.6 Mt (7.3 kg per capita) of e-waste was generated which is a very significant increase. These values will continue to grow exponentially due to the continuous high demand for portable electronics. However, with the increment in electronic waste, recycled e-waste had decreased comparatively. Only 17.4% of the generated e-waste was recycled, discarding approximately 57 billion valuable resources, that were used to manufacture electronic devices. Establishing these values through the last decade, it is expected an increase by nearly 40%, being predicted approximately 74.4 Mt of e-waste by 2030 [3].

The majority of e-waste generated in 2020 was originated from small types of equipment (22.1 Mt) such as monitoring devices, mobile phones, GPS devices, and personal computers [4]. Consequently, the production of these materials implies the usage of several critical elements namely mercury, lithium, or even some types of plastic, which are extremely toxic putting in danger to the environment and world population. According to a UN report of different industries, one worker dies every 15 seconds due to contact with harmful materials [5]. To prevent this paradigm, it is extremely urgent to stop this massive production and start adapting our society to nearly zero e-waste strategies along with the circular economy globally and especially in Europe, since it is the continent with the most e-waste generated in recent years.

[1] Valuable resources includes gold, silver, copper, platinum, and palladium.

## 1.1 Eco-design Strategies

Most of the e-waste generated, in recent years, was not taken into recycling procedures (less than 20%). Therefore, sustainable measures were implied, such as the Circular Economy (CE) which has taken an important stand in our society since 2015, regarding the economics in favor of the environment. The circular economy is a sustainable term where it prevents materials from being used in just one life term, providing a longer lifetime to diverse materials and products [6]. This practice is highly connected to eco-design strategies, where minimum resources are applied from ecological perspectives. This challenge demands the production of only essential and environment-friendly materials that can also have great potential for recycling and are capable of replacing others whose characteristics are a barrier of this mechanism, like plastic [7]. With plastic cost on manufacturing and recycling processes, its viable to strategize a climate action plan where these materials are replaced with eco-friendly raw materials such as cellulose and consequently paper, that can be used in different applications and principally avoid a climate negative impact and support this "zero e-waste" challenge [8].

**Figure 1.1** - Paper life-cycle from the raw material to the ecological energy devices (thesis work).

## 1.2 Paper in Electronics

With this new mentality of implementing the CE in our daily life, there is a challenge to adapt people's minds to finite natural resources so it can generate a positive cycle in a sustainable environment. This paradigm is caused due to the decrease of life cycling of products, mostly electronic in our daily life. The circular economy states that it is possible and must be done the maximization of resources and reduction of premature waste, by making the best usage of certain products. Having this mentality, it is certainly effective to connect all these principles with an eco-material as paper [9].

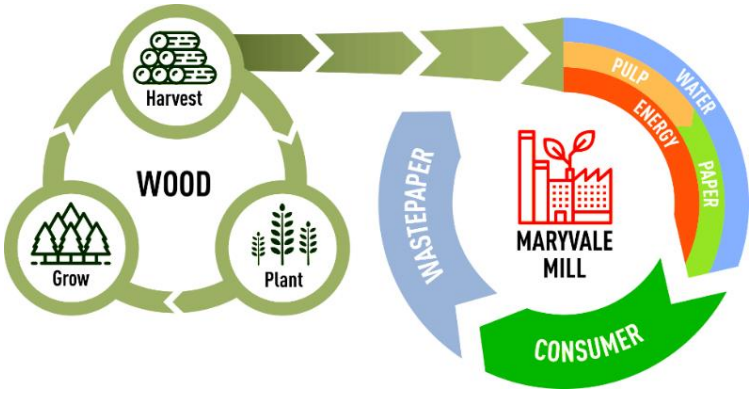


**Figure 1.2** - Paper recycling integration on Circular Economy.

It is well known that paper can be submitted to recycling processes several times due to Its mechanical properties [10]. Therefore, it is viable to combine paper with electronics to produce an alternative and sustainable feature that will impact our market and battle aside from the circular economy to a new ecological state.

Paper electronics is a field that is growing at a fast scale in the daily life of the world population. With its market availability and mechanical properties, paper is leaving its trace in other electronic fields. Recent studies have shown the potential of paper as the main substrate of supercapacitors [11], paper transistors [12], and electrode composites [13], where it seeks to find a pattern on having a sustainable substrate, recyclable and affordable, and effective as well on electrochemical interactions, during charging-discharging processes.

## 1.3 Polyaniline as Electronic Material

Polyaniline, also known as PANI, is a conjugated polymer with interesting properties, such as simple synthesis, high production yield, and electrical stability. PANI is a self-sufficient polymer, which means that does not need to be blended with other conventional polymers to alter its structure, providing the necessary structural stability to the matrix polymer [14]. PANI has already been reported as a promising functional polymeric material, that can easily be formulated with cellulose/paper substrates to synthesis highly efficient polymeric paper substrates [15]. In this work, recycled paper (RP) has been used to be functionalized with PANI through dipping in a polymeric solution, via suspension [16]. The functionalized RP (RFP) exhibits dark greenish-blue color, which represents the state of emeraldine, indicating a strong conductivity of the active layer.

Due to its interesting electronic structures, PANI has been investigated in different electronics applications such as supercapacitors [17], batteries [18], Polymer organic light-emitting diodes (PLED) [19], chemical sensors [20], biosensors [21], and biomedical [22] applications.

Interestingly, very recently, these conjugate materials were also investigated as mechano-responsive energy harvester applications, where these conjugated polymers initiate the charge transport mechanism under mechanical stress, which is able to generate electrical energy [23].
In this thesis work, PANI has been investigated through the functionalization of recycled paper into paper-based smart electronic applications such as energy harvesting and pressure sensors. The eco-design strategies of the functionalized recycled paper take the technology a step further in the area of sustainability and impact on zero e-waste challenge.

## 1.4 Electronic Paper for Smart Applications

### 1.4.1 Mechano-responsive Energy Harvester

With the current enormous commercialization, electricity has one of the highest levels of requirements. However, the conventional process of electricity production (mostly fossil-based) generates the largest share of greenhouse gas emissions [24]. Therefore, it is an urgent requirement to take steps towards green and sustainable energy applications. On the other side, with extreme use of small and smart electronic appliances, sources of energy need to be portable being able to feed electrical power uninterruptedly at the power levels of micro-to-milliwatts. Some relevant bioenergy scavenging technologies like thermoelectric [25], and mechanoelectrical (piezoelectric and triboelectric) [26], with the merits of flexible, high density of energy, and high sensing activity. Among them, mechano-responsive energy harvester is considered as one of the most interesting, because it can harvest energy from daily wastage of mechanical energy in form of any kind of motion, vibration, and touch, independent of seasons, weather, and position; it can be used spontaneously without using storage devices, which can be very useful for wireless signal mechanism or tracking system.
The core idea behind this mechanism is when two different layers come together and make a contact with stress (either rubbed/sliding or pressing), resulting in a current generation due to the charge transfer mechanism [23]. To increase the conductivity bridge between layers, conjugated polymers (CP) are a new low-cost option. The energy harvesting abilities of conjugated polymers are based on the energy-transfer process through the π—π* interaction in its backbone, which can easily be modulated through a simple doping process. **Figure 1.2** shows the schematic representations of the charge transfer mechanism. Recent studies have shown the potential of paper/cellulose substrate to design triboelectric nanogenerators as sustainable power sources [27], [28], capable of generating an electrical output via finger touch. One step fruition to the sustainable goal, in this work, we have used recycled paper for fabricating this energy device.

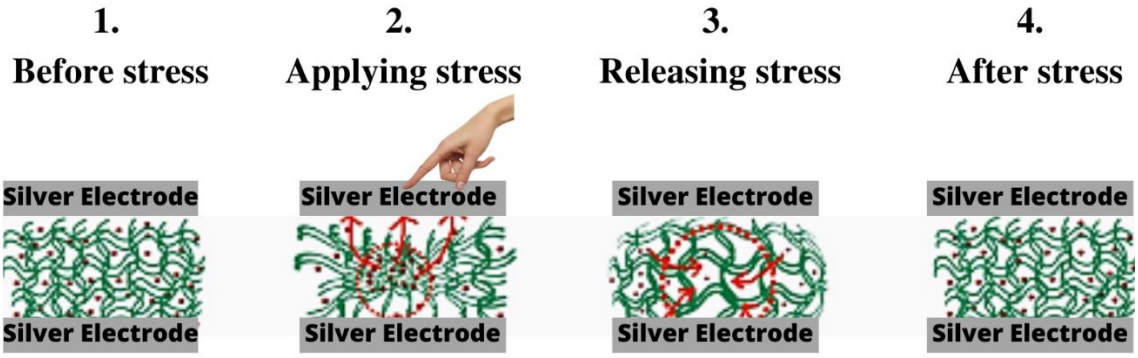


**Figure 1.3** - Mechano-responsive charge transfer on PANI recycled cellulose.

### 1.4.2 Pressure Sensors

Energy storage devices are trending in this scientific area due to their capability of saving energy while being pressured with charge-discharged cycles and good stability, retaining most of the specific capacitance. Supercapacitors (SC) are replacing batteries since they have much more power density, life cycle, and safety than conventional batteries [29]. Uno, et al, (2012) reported, that SC´s are cycled in low-currents when put into charge-discharge processes, thus yielding an adequate power capability.

In the field of energy-storing and energy harvesting, pressure sensors devices with paper-based active substrates are immerging. The core idea of applying these flexible and wearable pressure sensors is to replace conventional ones that fail in achieving good sensitivity on a wide working range. The bonding of conductive polymers and electrodes with a paper-based substrate has shown great piezoresistive performances [30], [31]. Lu-Qi et al (2017) [30] used graphene-oxide as a conjugated polymer to apply pressure sensors in different tests, to compare the pressure sensors' performance on different vibrations. Applications such as wrist pulse and breathing detection on different occasions demonstrated a good pressure range of 20 kPa and high sensitivity between 0 and 2 kPa with great flexibility and stability simultaneously.

In recent studies [32], [33] it is investigated the application of PANI as conjugated polymer on smart ecological pressure sensors, achieving good sensitivity and voltage decrease when applying pressure. Drishya et al (2021) [16], reported excellent performances of polyaniline as a conductive polymer for pressure sensors. The cellulose/PANI-based piezo-resistive sensors exhibited great output levels due to the conductivity of the active layer. The pressure was conducted only with external compression directly on the multilayer sensor, registering a high sensitivity of 2.23 $kPa^{-1}$, a pressure range between 2 and 90 kPa with a fast and stable response of 70 ms on up to 800 cycles [16].

# 2 MATERIALS AND METHODS

In this chapter, it was addressed the methods and materials used for the recycling and treatment of the wastepaper into new paper substrate (Recycled paper, RP), the fabrication and functionalization of the RP, and the eco-design of smart devices fabrications (energy harvester, pressure sensor) using functionalized RP (RFP). In all the device fabrication, RFP has been used as an active layer. All reagents used in this thesis, are reported in section 2.1. The characterization methods used are also described in section 2.4.

## 2.1 Reagents

The main goal of this thesis is to use newspapers to produce new matrices for sustainable electronic devices. Thus, cellulose from newspapers was the main material, to be furtherly recycled and re-used on different methods.

To produce the RP it was considered three reagents, that were used differently depending on the sample: sodium chloride (NaCl; ≥99.0%, ACS reagent, Sigma-Aldrich), citric acid (CA; 99.5%, Sigma-Aldrich), and sodium dodecyl sulfate (SDS; ≥99.0%, ACS reagent; Sigma-Aldrich).

Meanwhile, the synthesis of the polyaniline (PANI), that was obtained to functionalize the samples, using for the synthesis the following reagents: aniline (AN; 99.5%), ammonium persulfate (APS; 98.0%), camphor-10-sulfonic acid (CSA; 98%, Sigma-Aldrich) and hydrochloric acid (HCL; ≥37%, Sigma-Aldrich).

All the recycling and functionalization methods were carried out in a low-cost technique. Furthermore, for smart device applications, screen printed silver/carbon layer has been used as an electrode layer.

## 2.2 Recycling of the Newspaper

The used newspaper was treated and recycled to be used as the main substrate. To achieve the eco-design wanted for the devices, different but simple procedures were put into practice to achieve the purpose. The newspaper was cut into small pieces and immersed in deionized (DI) water to soak the fibers and help with their separation. Thereupon, the paper was poured to obtain a uniform paper pulp, and the water in excess was filtrated with an 800 μM drainer, to prevent pulp loss. Furtherly, small pieces were formed and squeezed, to be further cut off and dried in the hoven at 60 ºC for 24 hours. After dried, the pulps were blended again to obtain the small flakes (i.e., as recycled cellulose fibers) that were posteriorly used on samples.

## 2.3 Fabrication of Recycled Cellulose-PANI Electronic Devices

### 2.3.1 Recycled Paper Fabrication

After the dispersion of the cellulose fibers in DI water (160 ml) with the help of a blender, it was used a Sonicator (Sonics VCX 750, 13mm), an ultrasonic liquid disperser, to separate the fibers. Simultaneously, the solution was taken into a continuous stirring of 500 rpm at room temperature. After filtration, the cellulose was placed on a polystyrene Petri dish with an approximate volume of 43 $cm^3$, that was reused. The samples were dried in the laboratory oven at 60 ºC for one full day. Posteriorly, after complete drying of the paper, all samples were removed from the Petri dish and characterized.

### 2.3.2 Functionalization of Recycled Paper

For the synthesis of PANI, the reagents that have been used are mentioned in section 2.1. To synthesize the Emeraldine state of the PANI, two solutions (named as solution A and B) were made. Solution A was prepared with 0.928 g of APS dissolved in 10 ml of DI water and solution B, with 0.4646 g of CSA dissolved in 20 ml of DI water. After 10 minutes of steering agitation (450 rpm) of both the solutions, it was added 100 µl of HCl and 365 µl of Aniline were added to solutions A and B, respectively. The solution was then agitated again for 10 minutes to homogenize the chemicals before the functionalization of RP. For polymerization from aniline to polyaniline, solution A was added directly to solution B, at room temperature. After mixing both samples, it took around 5 minutes for the samples to change into the desired color (dark greenish-blue which indicates the polyaniline phase). All the RP samples were immersed into the polyaniline solution for 2 minutes to functionalize the sample. The functionalized RP (RFP) was then dried in room temperature and prepared for chemical analysis and device fabrication. **Figure 2.1** shows the schematic illustration of the chemical synthesis and **Figure A.1** (in the annexes) shows the real images of the step-by-step chemical procedure.

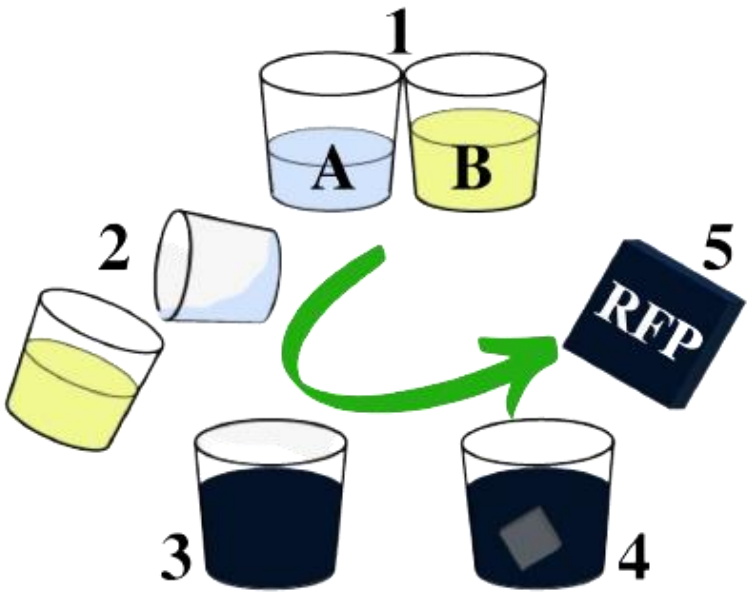


**Figure 2.1** - Functionalization via suspension (deep-cast method). 1– Solution A and B with respective chemicals; 2- Solution A mixed on solution B in a 1:2 ratio; 3-Synthesized Polyaniline (emeraldine): dark greenish-blue; 4- immersion of the samples on the solution (2 minutes); 5- RFP sample functionalized after dried at room temperature.

### 2.3.3 Fabrication of Electrodes

The flexible electrodes layers for the smart device's fabrication were produced by screen-printing, using silver ink (CRSN2442 AG INK, Coated Screen Inks). The ink was printed on Whatman paper (Whatman™, Chromatography Paper, Grade: ICHR) fabricating several electrodes, and dried on a hot plate at 100 ºC for about 30 minutes. These electrodes will integrate the cellulose-PANI layer as a charge collector. The silver electrodes are shown on the Annexes, **Figure A.2**.

### 2.3.4 Fabrication of the Eco-smart Devices: Energy Harvester and Pressure Sensors

The eco-energy devices were designed with a ecological footprint, where the RFP was used as active layer (AL) and silver electrode was used as charge collector layer (CCL). The device functional mechanism has been explained in section 2.3.3. AL layer was connected directly to the charge collector layer (CCL), which is the silver electrode, on both surfaces, also two copper tapes were connected on each side two prevent CCL. All the layers are fixed with commercial tape, to provide the necessary stabilization to the device. All the devices had the same size and shape, with a 4 $cm^2$ AL. In **figure 2.2** is illustrated the device structure with respective layers.

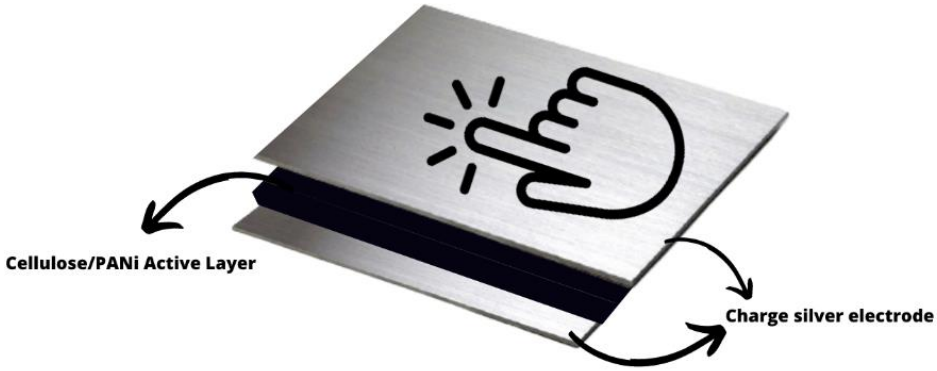


**Figure 2.2** - Illustration of the layers montage on the eco-smart devices for energy harvesting: Two charge collector layers (CCL) of silver and one active layer (AL) which is the functionalized cellulose sample. Both layers were encapsulated with commercial tape and two copper tapes were connected on the sides to prevent damage to the CCL.

## Pressure sensors

The resistive pressure sensor devices were fabricated very similarly to the devices produced for energy harvesting, although some significant changes were made to improve the electrical output when applying pressure. Thus, one of the faces of the functionalized paper with doped polyaniline was screen-printed with silver ink while the opposite face was placed on top of silver ink printed on the Whatman filter (electrode). For the encapsulation, the method is similar, where white paper and tape were used to properly fix the substrate.

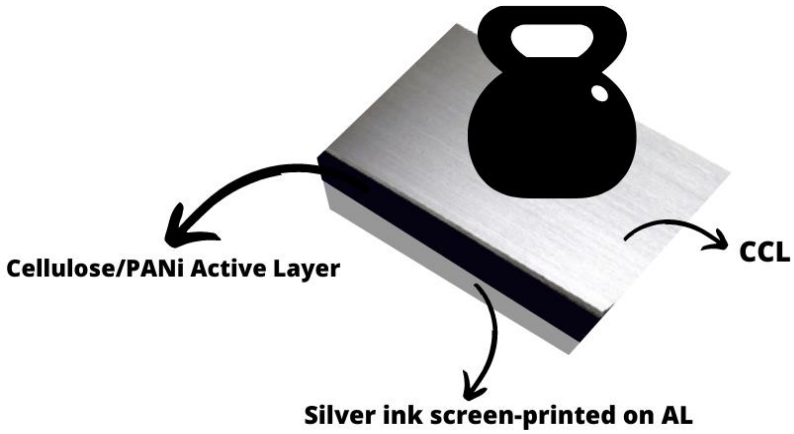


**Figure 2.3** - Illustration of the layers montage on the eco-smart devices for resistive pressure sensors: One charge collector layer (CCL) of silver and one active layer (AL) screen printed on one surface with silver ink. Both layers were encapsulated with white paper and commercial tape.

## 2.4 Characterization Techniques

### 2.4.1 Morphological, Chemical, And Compositional Characterization

To determine all the morphological, chemical, and compositional properties of the samples, before and after functionalization, it was used several characterization tools. The morphological analyses of the cellulose fibers were made by a Scanning Electron Microscope (FESEM, Hitachi TM3030 Plus) while the elemental composition of the samples was analyzed via energy dispersed X-ray spectroscopy (EDX).

### 2.4.2 Optical Characterization

Fourier-transform Infrared spectroscopy (FTIR, Thermo Nicolet 6700 Spectrometer) was used to perform chemical analyses of the samples, before and after polymerization. Attenuated total reflectance (ATR) was applied, with a spectrum (wavenumber) between 500 and 4500 $cm^{-1}$.

### 2.4.3 Electrical Characterization

The electrical characterization of the polymerized samples was conducted using a Hall effect system to measure the sheet resistance and Hall mobility of the functionalized samples.
Meanwhile, the characterization of the energy devices was done by measuring the mechanical impulses generated on the device with the assist of a standard oscilloscope, (Tektronix TBS 2022). The voltage values obtained from the mechanic pulses were later transformed to current and power density values. The analytical data from the resistive pressure sensors were recorded through Arduino-customized electrical measurement setup system.

# 3 RESULTS AND DISCUSSION

This chapter presents and discusses the work done for the production of ecological energy devices and paper-based pressure sensors, from recycled newspaper to their characterization, all made with a sustainable mindset.

Firstly, in section 3.1, the recycling process from the used newspaper to obtain the cellulose fiber flakes is explained in detail. Secondly, section 3.2, is dedicated to the production of the recycled samples and their morphological analysis. Section 3.3 deals with the polyaniline and the polymerization of the samples, being described all methods and characterization. In section 3.4, the ecological energy devices are analyzed and their electrical output performance and applications on powering up LEDs are studied. At the end of this chapter, it is explained in section 3.5 the process of the ecological functionalized paper applications on the fabrication and electrical characterization of recycled paper/PANI-based pressure sensors.

## 3.1 Recycling Of The Newspaper

Newspaper is heavily used in daily life as part of printed information, daily, weekly, or monthly. Even in the age of electronic media, newspapers are still having its own market. As Newspaper is mostly designed by mixed of new and some sort of recycled cellulose fibers. Since it is printed paper, several ink chemicals and fillers are present in the newspaper.

The recycling of paper is a well-implemented process in the daily life of the world population. Currently, paper is emerging as a product with the potential for replacing materials, like plastic, due to its environmental footprint and economical value. Recent scientific publications [34]–[36] reported studies on the pulp properties and quality after recycling processes. Alina, et al (2010) [34], analyzed recycled newsprint surface when mixed with packaging paper, concluding on an improvement of the physical properties when using a flotation process, which removes most of the ink present at a fastest pace. In the present work, flotation of the wastepaper fibers is applied to decrease the fillers and ink chemicals present on the newspaper, as well as using the same paper type throughout the process, to avoid contamination.

Also, pulp drying is a really important step for this recycling phase [37]. Therefore, two different processes were used to see the most efficient method for wastepaper recycling: the soaked pulp was alternatively dried at room temperature and dried on an oven, at 60 ºC for 24 hours. It was verified that when completely dried each sample, the first divergences between both processes were the drying time and the thickness of the cellulose flakes. The natural drying method was a slower process, resulting in thicker and more rigid cellulose flakes compared to the other

method. Therefore, oven drying was selected as the principal process of drying the recycled newspaper. **Figure 3.1** shows the newspaper that has been used for recycling and the pulp after the recycling process.

**Figure 3.1 -** Newspaper and fibers obtained during the recycling process.

In this study, two types of newspaper were treated before proceeding to the fabrication of the samples: color paper and black and white (BW) paper. Although along the process no variability was clear between both substrates, after drying, the color paper was much rough and reddish than the BW paper. These differences between the substrates, lead to conclude that BW paper has less variability and was more effective to be used as the main substructure for the fabrication of the ecological energy devices. A step-by-step of the recycling process can be seen in **Figure B.1** of the annexes.

## 3.2 Samples Fabrication

### 3.2.1 Selectivity And Processing

To produce the recycled newspaper, several trials were made using different percentages of chemicals and cellulose to achieve the cellulose matrices with desired properties to be used for the devices. Therefore, the characteristics required for the samples were: flexibility, sponginess, and resistance. Using the results used in a recent study [38], it was obtained a 3 w/w%, of cellulose on the first samples. It was established 5g of cellulose, therefore it was diluted on 162 ml of deionized (DI) water. For the reagents, it was used 0.25g (100 g/L), 2.922g diluted in DI water (0.1 M) and 0.015g (3 g/L) of citric acid (CA), sodium chloride (NaCl), and sodium dodecyl sulfate (SDS), respectively. The core idea of using these reagents was mostly for

bonding, foam formation, and density stabilization. CA is an affordable non-toxic polycarboxylic acid (PCA) generally used to increase the stability and strength of materials in water, generating hydrophobic properties. This PCA had an important role since it increases the cross-linking of the cellulose, strengthening the fibers [39]. The usage of SDS targeted the improvement of morphological properties of the cellulose matrices, given that it is a foam-forming agent. Finally, NaCl as a bonding agent has the applicability of bonding the cellulose fibers and the involved reagents.

The NaCl was used only in one sample. The sample with the salt ended up having the best electrical performance on the energy devices, possibly due to the density increase and ionic dissociation from the salt, which improved the energy transfer of the mechanical stimulus.

With the 3 w/w% mentioned above, the cellulose samples were drained to a cylindrical mold and dried in the laboratory oven at a temperature of 60 ºC. In these trials the pH was stable (pH =6.5), not lowering as expected with the addition of the citric acid, this being caused probably by the high percentage of lignin and fillers on the cellulose sample, making it difficult for the chemical to blend in. After that, the amount of cellulose was reduced to 1 w/w% to the same volume of water (162 ml) using the same masses of the chemical reagents mentioned before. With this weight of cellulose, the pH decreased to 3.5 but the cellulose sample after drying was still stiff and easy to break if bent.

Due to that, it was made a replacement of the molding and a decrease of the cellulose. Two percentages of 0.5 w/w% (0.83 g) and 0.2 w/w% (0.32 g) were tried with a new filtration. This filtration process is a simple drop to mold casting where the solution is poured into a PS Petri dish as the excess water was filtrated with filter paper. The 0.32 g was too fragile; thus, it was disregarded. The samples prepared with 0.83 g were satisfactory presenting exceptional flexibility, adequate sponginess, and a smooth surface.

### 3.2.2 Measurements and Morphological Analysis

The reagents were tested on recycled cellulose samples resulting in four final samples (**figure B.2**, on the Annexes) that were reproduced constantly throughout the rest of this thesis work for electrical analysis and devices applications.

All the RP samples were fabricated with 0.5 w/w% of cellulose for 165 ml of DI water. Yet different chemicals were added to the samples to analyze and compare the resulting morphological and mechanical properties, except for RP4, which was processed only with cellulose fibers:

- RP3 was the only sample processed with sodium chloride.

- RP1, RP2, and RP3 had citric acid (CA) to increase the strength between the fibers and decrease the solution pH to facilitate the polymerization process.
- RP1, RP2, and RP3 were fabricated with different portions of sodium dodecyl sulfate (SDS) used as a foam trigger to the samples sponginess and texture: 0.015 g on samples RP1 and RP3 and 0.075 g on sample RP2.

The core idea of these quantities was simply to compare the performance of the samples on different hypotheses. Table **3.1** are indicated all the reagents and respective quantities applied to each sample. Samples measurements and properties are listed in **table 3.2**.

**Table 3.1** - Reagents quantity on all samples.

| SAMPLE | CELLULOSE (g) | CA (g) | SDS (g) | NaCl (g) |
|---|---|---|---|---|
| **RP1** | 0.83 | 0.25 | 0.015 | - |
| **RP2** | 0.83 | 0.25 | 0.075 | - |
| **RP3** | 0.83 | 0.25 | 0.015 | 2.922g dissolved in 5ml of DI water |
| **RP4** | 0.83 | - | - | - |

**Table 3.2** - Recycled paper (RP) samples characteristics.

| SAMPLE | THICKNESS µm | g/cm$^2$ | THEORIC DENSITY (g/cm$^3$) | DENSITY (g/cm$^3$) | POROSITY (%) |
|---|---|---|---|---|---|
| **RP1** | 871 | 0.019 | 1.60 | 0.22 | 86.3 |
| **RP2** | 832 | 0.017 | 1.58 | 0.21 | 86.7 |
| **RP3** | 1261 | 0.04 | 2.00 | 0.31 | 84.5 |
| **RP4** | 722 | 0.019 | 1.6 | 0.27 | 83.1 |

Furthermore, to analyze the morphological properties of the RP samples, SEM imaging of the cross-section was conducted on all samples to compare the effect of the chemicals on the fibers. **Figure 3.2** shows the matrix of the samples fibers and a surface photograph of each paper.

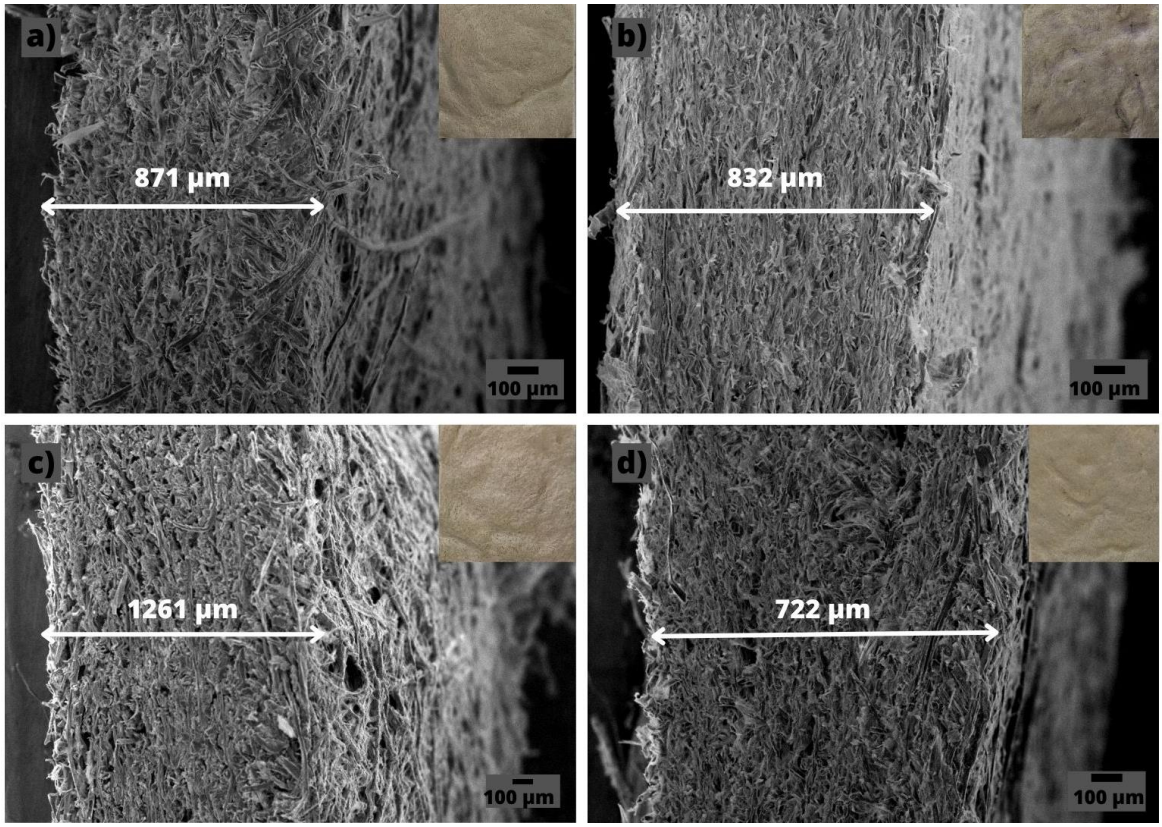


**Figure 3.2** - SEM morphological analysis of the RP samples cross-section (1mm) images. Images a), b), c) and d) correspond to samples RP1, RP2, RP3 and RP4, respectively.

The distribution of the fibers is more uniform on RP2 and RP3 with more unidirectional oriented fibers.

When analyzing RP1 and RP4, more dispersion and lost fibers, as well as gaps between the fiber walls are found, which is even more clear on RP4 what can be explained by the absence of any chemicals reacting with the cellulose. In contrast, when using CA, which strengths the cellulose networking, a slight increase in the uniformity of the fibers can be observed.

When the SDS was increased five times on RP2, a significant change in the orientation of the fibers and sponginess compared to RP1 was observed due to the increase of the sample foam. However, when analyzing the snapshots between RP1 and RP2, it is evident the much darker and stained paper of RP2. This suggests that the increase of the SDS quantity should be further investigated if bleaching chemicals, such as sodium chlorite e.g., are used.

The density of RP3 stood out from the other samples by an additional ~30% due to the NaCl performance as a bonding agent. In **figure 3.2c** it is observed less space between the walls of the pores with no dispersed fibers. Both microscopy images are very similar to sample RP2 **figure 3.2b** what suggests the positive bonding effects of the NaCl with higher SDS on further investigation of ecological energy devices and harvester pressure sensors.

## 3.3 Cellulose Samples Polymerization

Although several conjugated polymers can be used on the samples polymerization, it was selected polyaniline (PANI) due to its availability and high performance in most environments and materials. The functionalization of the samples with the PANI was tried out with two different syntheses. At first, the synthesis was executed with a two-step drop-casting method with the same reactions mentioned in section 2.3.2. However, the emeraldine phase from polyaniline was not verified. To overcome it, since the cellulose samples were made with recyclable paper which contains fillers, ink, and other additives, it was effective to use a suspension method (**Figure B.3**, annex section B) for the PANI to achieve an emeraldine state that is known for its semiconductor properties. With this method, the PANI filled inwardly all the samples, providing their complete functionalization of the samples.

### 3.3.1 Chemical and Morphological Analyses

As mentioned above two methods were used to functionalize the RP samples with PANI. The first method was used in previous studies [15, 23], to functionalize pure Whatman paper and nano textile fibers. However, when experimented on recycled paper, the two-step drop-casting method was not as effective as on the filter paper. In this process, a mixture of solutions A and B (described in section 2.3.2) in a ratio of 1:2, respectively, was drop cast on one side of the paper. To each sample (2x2 $cm^2$), it was applied an amount of 24 μL of solution A and 48 μL of solution B. After 10 minutes at room temperature, the polyaniline oxidation on the paper was not effective inward the sample. To overcome it, a deep-cast method via suspension was used (materials and method, section 2.3.2). As the PANI was absorbed on the fibers and the doped emeraldine phase was confirmed, the samples were dried at room temperature, to be further characterized. In this process, the RP samples were suspended on the polyaniline semi-conducting reaction, achieving the full functionalization of the paper, even with the higher porosity (82 to 87 %).

To observe both PANI functionalization on the RP samples and compare both methods effectiveness, several SEM images were obtained to characterize the presence of the polyaniline on the fibers and its structure. In **figure 3.3**, it can be analyzed the SEM images and an up-close snapshot of the functionalization processes of each sample, wherein a) corresponds to the one-step drop-casting method and b) to the suspension/deep-casting one. On both methods, it was used a ratio of 1:2 of solution A:B. However, the drop-cast method wasn´t effective in involving the fibers inwardly, possibly due to the porosity and thickness of the paper, since it is a slow absorption substrate. In **figure 3.3a** it is visible the lack of PANI into the cellulose fibers matrices and the greenish-yellow color both confirm that the emeraldine phase of PANI was not

achieved. Nonetheless, in **figure 3.3b** due to the effectiveness of the polymerization of the RP via the deep-casting method, it is observed the presence of polyaniline in between the cellulose fibers matrices, what is normally microscopely identified as small particles that form isolated granules on the fibers [40]. In **figure B.4**, on the Annexes is a snapshot of both functionalization methods.

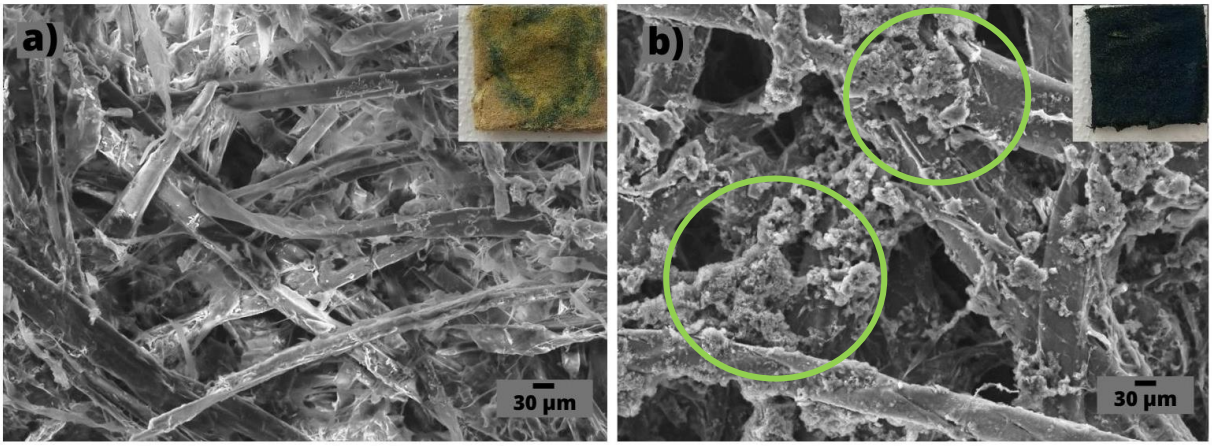


**Figure 3.3** - A comparison of both functionalization methods via SEM (scale of 300 µm) and a photograph of each sample. a) two-step drop-cast method; b) suspension/deep-cast method. On a) the functionalization was not achieved as seen by the absence of PANI on the fibers and the yellow color of the samples, on the contrary b) presents a dark greenish-blue color which confirms the presence of emeraldine salt.

When analyzing the functionalized RFP samples via SEM Imaging, in **Figure 3.4** it is possible to observe a significant difference in the PANI polymerization between each sample surface. Samples RFP3 and RFP4 achieved a better superficial and internal functionalization on the paper fibers, with polyaniline granules, homogenously spread. Although it is possible to see some functionalization on paper RFP1 and RFP2, both lack PANI, especially sample RFP2. It can be explained by the excess of foam formation due to the increase of SDS.

Analyzing the structure of the fiber matrices, RFP3 was the most unidirectional one with fewer holes between pores walls, caused by the increased density triggered by the NaCl. In **figure 3.4d** sample RFP4 presents an unorthodox matrix, with the bigger space between fibers due to no chemical interaction, however, it is possible to observe the functionalization inside of the cellulosic structure. Additionally, sample 4 had the best surface smoothness following sample 3.

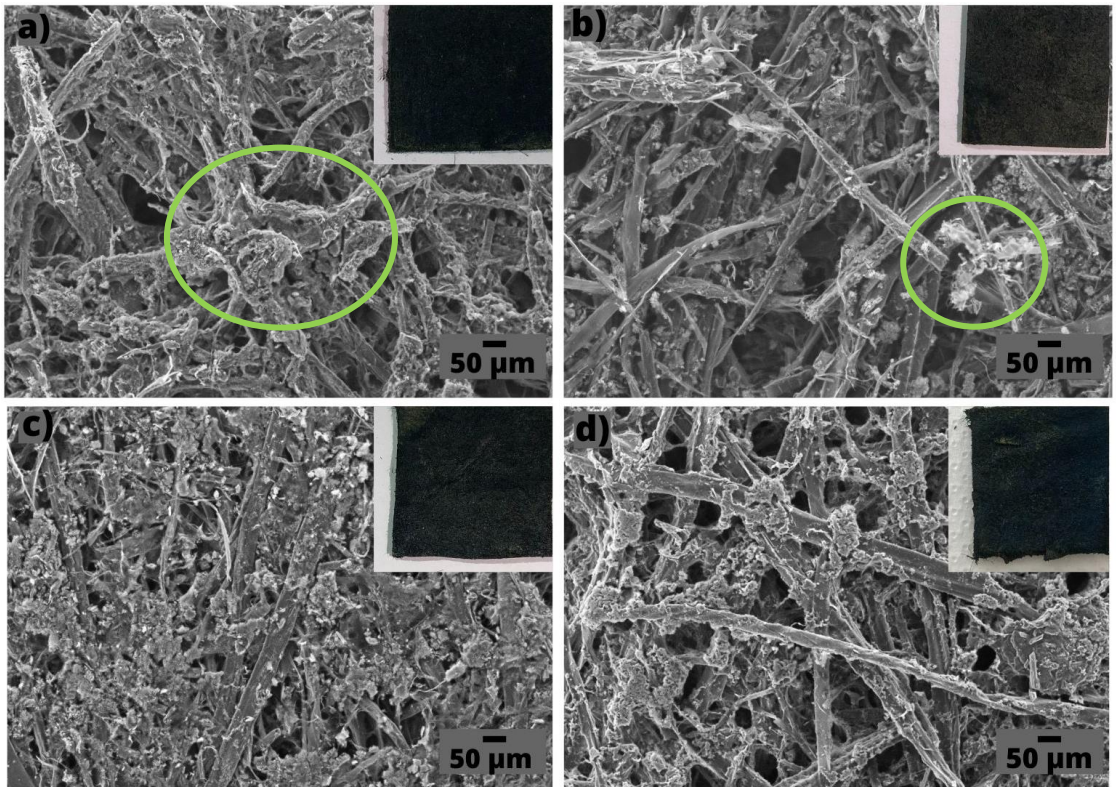


**Figure 3.4** - SEM Image of all functionalized samples with PANI with suspension/deep-cast method. a) RFP1; b) RFP2; c) RFP3; d) RFP4. In the inset is presented a photograph of each sample.

An Energy-Dispersion Spectroscopy (EDS) elemental mapping was performed in association with the SEM scanning. The EDS was performed to analyze the chemical composition of each functionalized sample. In the EDS mapping, all samples were composed of the same elements. Carbon and oxygen are the two most abundant elements on the samples (~90%) due to the substrate structure, which is mainly cellulose. Also, sulfur and chlorine are mapped in the chemical composition in a small percentage. The mapping of this element indicates the presence of the $Cl^-$ anion from the hydrochloric acid and CSA, as doping agents [41]. In addition, the analysis proves the polyaniline formation on the cellulose sample.

To chemically analyze the samples before and after functionalization, a Fourier-transform infrared (FTIR) spectroscopy was performed. This technique is an effective infrared method that can identify specific functional groups present in a sample by absorption and detection of radiation due to the excitation of molecular bonds on the cellulose. In this study, due to the highly absorbing samples, FTIR was performed with Attenuated total reflectance (ATR) which is a non-destructive method that allows attenuation of the radiation, which provides several absorbance peaks in different spectra [42].

To observe the changes in specific patterns of the chemical composition of the samples, all of them were analyzed before and after functionalization, on ATR-FTIR to compare the changes

in the morphologic composition after the doped polyaniline. Each sample was analyzed on the upper surface to prevent misleading measurements between them. ATR-FTIR analyses are shown in **figure 3.5**, where different peaks can be retracted and analyzed. In each graph, the spectra curves of each sample surface before and after functionalization are registered.

At first, three bands that confirm the presence of cellulose can be observed on both spectra of the recycled wastepaper: The peak of the C-H stretching vibrations (2900 $cm^{-1}$) due to the general organic content present on the samples, and the peak of the C-O-C band and C-C ring breathing (1150 $cm^{-1}$) authenticates the presence of cellulose fibers on the recycled paper on both phases [43]. Although these peaks are observed on both phases, the peaks intensity after polymerization decreases since most of the cellulose fibers are covered with polyaniline, lowering the values of cellulose detected from the reflected IR spectra.

When analyzing the spectra generated by the PANI, five peaks stand out compared to the pre-functionalized paper. The peak at 807$cm^{-1}$, C-H bond, manifests the benzene circle of PANI stretching vibrations and the peak of 1122 $cm^{-1}$ represents the quinoid band, -N=Q=N-, stretch vibration. The C-N bonds on peak 1304 $cm^{-1}$ corroborate the stretching of the benzenoid rings of the PANI. At least, C=C bands are spotted on both curves with two peaks between 1480 and 1580 $cm^{-1}$, which indicates the presence of lignin on the fibers of the wastepaper and the stretching of the quinoid and benzenoid rings in the doping of the conjugated polymer [44].

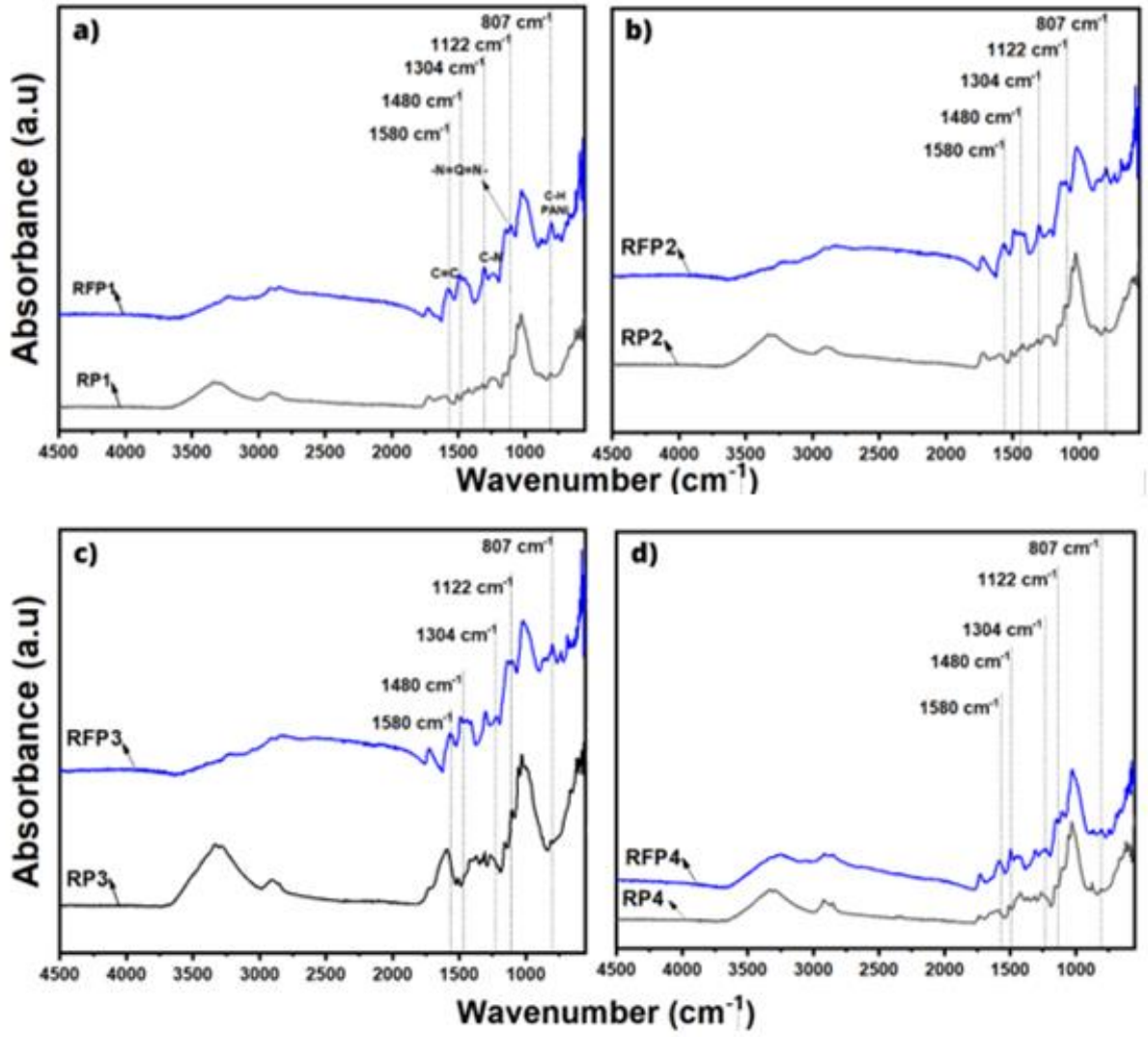


**Figure 3.5** - Comparison of ATR-FTIR spectra curves before and after functionalization of each sample; Spectra for pristine and PANI functionalized samples: a) RP1 and RFP1 spectra with the PANI bands with correspondent designation (same on the other graphs); b) RP2 RFP2; c) RP3 and RFP3; d) RP4 and RFP4. The dashed lines are related to the characteristic PANI absorption bands present for every RFP sample spectrum.

### 3.3.2 Electrical analysis

The electrical characterization of the functionalized samples, namely the electrical charge distribution and sheet resistance, was made in Hall effect equipment. All measurements were performed in a Biorad HL5500 Hall effect equipment (**figure 3.6**) with a permanent magnetic field of 0.5 T at room temperature (pre-established). This system is a high-performance system with a four-point probe technique capable of measuring the resistivity and Hall mobility of the samples.

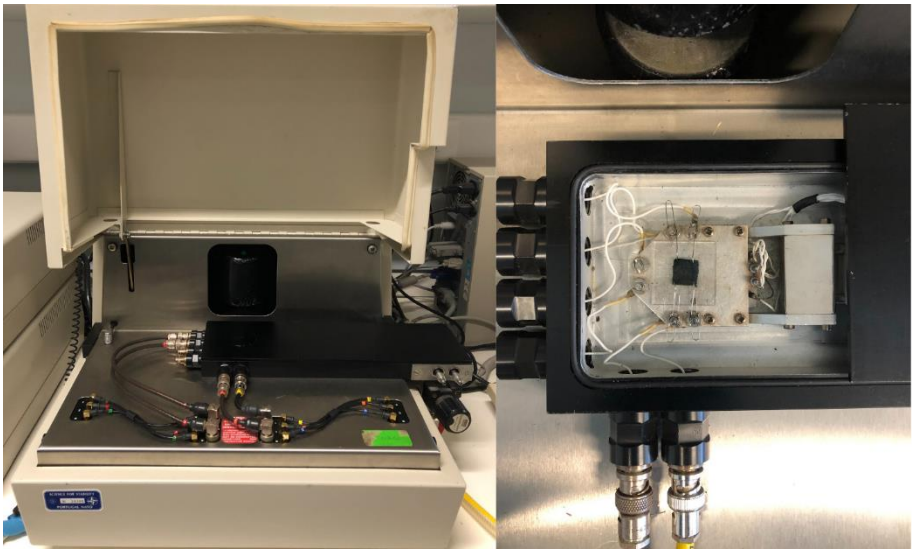

**Figure 3.6** - Biorad HL5500 Hall Effect System (HES) and an example of a sample setup with the four-probe pointers fixed on each edge of its.

The measurements on this analysis are to characterize the electrical properties on the surface, thus only sheet resistance and hall mobility were considered for this study. Since the samples had different geometry, that causes a different thickness on the same sample, resulting in inconclusive bulk results. In **table 3.3**, all measurements are registered.

The electrical parameters were measured at room temperature, with a fixed magnetic field, meaning that the resistivity and mobility measured on the surface will be analyzed as equal. This strong magnetic field will disturb the charge carriers directions, deflecting both positive and negative charged electrons in different ways, generating a potential difference (Hall voltage). This magnetic force applied on charge carriers orientation is named Lorentz force [45]. For all functionalized samples an average current of 5 µA was applied. When analyzing the sheet resistance ($R_{sh}$) of all RFP samples the values were high, which can be explained by measurements errors due to the poor symmetries of the samples surface, since the polymerization of the samples was achieved.

Dhawale, et al (2009) [46] reported the sheet resistance of doped polyaniline on nanofibers, concluding with an average $R_{sh}$ of 4.04 Ω. Also, it was measured a high hall carrier mobility of 549.35 $cm^2$/V-s. The usage of doped PANI on the nanofibrous films was more effective compared to the recycled wastepaper, due to the mechanical properties of the different substrates. Although these matrices are highly porous, like the RFP samples, the deposition of only polyaniline thin films directly on the nanofibers, can highly influence the electrical performance of the conjugated polymer. To assist this theory, a previous study [47] measured the resistance of doped polyaniline films, synthesized with the same oxidants as the RFP´s with a four-probe

point. The sheet resistance was measured directly on PANI-based films, registering an Rs of 64.95 Ω proving that the resistance is influenced by the substrate morphological characteristics. Even with the significantly high resistance, the results between samples were expected. RFP2 and RFP3 have shown respectively the highest (3860 Ω) and lowest (670 Ω) sheet resistance, respectively. These measures corroborate the RFP samples morphological properties analyzed on SEM (**figure 3.4**).

As a complement to the resistance of the polymerized paper, Hall mobility (μH) was measured. When comparing the hall mobility, it is noted an average of high charge carriers mobility on all samples, with higher mobility on RFP3, which can be explained due to fibers uniformity observed on SEM imaging. The mobility obtained on the samples can be compared to recent studies [48], [49], where doped polyaniline was used on nanocomposites achieving carrier mobility of approximately, 50 $cm^2$/V-s. When analyzing the SDS influence on the electrical performances, it can be observed the low mobility on sample RFP2, with the highest amount of the surfactant solvent. Since SDS is a foam-forming agent it will form voids between the fibers, generating barriers for the movement of the charge carriers. This can be efficient for mechanical endurance, yet it will affect the electrical properties of the polymer. Cho, et al (2015) [50] reported the efficiency of different solvents on the charge-carrier mobility on polymeric semiconductors concluding on the lowest performance on SDS-based transistors ($10^{-3}$ $cm^2$/V-s).

**Table 3.3** - Electrical properties of all samples surface measured with a Hall Effect System (HES).

| SAMPLE | SHEET RESISTANCE ($R_{SH}$) (Ω $cm^2$) | HALL MOBILITY (μH) ($cm^2$/V-s) |
|---|---|---|
| **RFP1** | 2870 | 54.1 |
| **RFP2** | 3860 | 1.41 |
| **RFP3** | 670 | 163 |
| **RFP4** | 3180 | 75.2 |

## 3.4 Functionalized Energy Devices

After successfully producing and functionalizing the RP samples, a new challenge of fabricating sustainable energy devices was pursued. These devices were built to perform as energy generators, meaning that, through mechanical impulses, electrical energy will be generated through a charge transfer mechanism. The core idea of this process is to use functionalized paper, which due to the conjugated polymers, can transfer potential energy using mechanical stimulus.

Each ecological device was built with the same methodology, mentioned in section 3.3.4, where the functionalized cellulose sample, becoming an active layer (AL), was fitted between two silver electrodes, that will work as charge collector layers (CCL) and copper tape on both sides, to ease the semiconductive passage between electrode and oscilloscope, and to decrease the damage of the charge collectors. All layers were properly fixed to avoid displacement and misleading current measures.

### 3.4.1 Electrical Analyses

To compare all devices output performance, several electrical characterizations were performed. All the eco-energy devices had the same area of 4 $cm^2$ and the silver electrode was used as a CCL. All the devices were comparatively analyzed based on the open-circuit output voltage ($V_{oc}$) and short-circuit output current ($I_{sc}$) using an oscilloscope. For $V_{oc}$, the output of the eco-energy device was directly connected to the oscilloscope. For $I_{sc}$ measurement, a customized short circuit was used prior to the oscilloscope connection. An image of both circuits can be seen in **Figure B.5** of the annexes. Furthermore, the power density of all devices was calculated and compared, against external load, from 100 kΩ to 100 MΩ. During all the measurement applied force frequency and amplitude was kept unaltered.

**Electrical output performance**

To evaluate output electrical measurement ($V_{oc}$ and $I_{sc}$) value from each device (RFP1, RFP2, RFP3, RFP4), around nineteen mechanical stimulus pulses were exerted. This process was repeated five times for all devices to check their stability. An average of each device's output performance can be observed in **table 3.4**.

**Table 3.4 -** Average output voltage on open circuit ($V_{oc}$) and output current with a 100M ohm load resistance on a short circuit ($I_{sc}$); (energy harvesting with mechanic stimuli).

| DEVICE | OPEN CIRCUIT, $V_{OC}$ (V) | SHORT CIRCUIT, $I_{SC}$ (µA) |
|---|---|---|
| **RFP1** | 17.0 | 1.08 |
| **RFP2** | 15.6 | 0.86 |
| **RFP3** | 19.1 | 1.56 |
| **RFP4** | 17.2 | 0.87 |

The output performance of the device´s voltages was directly registered on a time vs. voltage plot, whereas for the current output since it was used a resistance of 100MΩ, the values were

calculated (V = RI). The voltage output did not differ significantly on all devices, reaching values between 15 and 20 V. The devices that had the lowest and highest output performance on both circuits were RFP2 and RFP3, respectively. Since the samples have differed on the solvents used, it was expected to have significant changes between them. Hence, this electrical performance is anticipated since RFP3 had a much more stable structure due to the bonding properties of the NaCl, whereas on RFP2 the foam increase had affected the PANI doping inward the fibers, as explained in section 3.3.2. RFP1 device fulfills the expectation, with average output values since it had the default amount of SDS (0.015g) without NaCl.

In **figure 3.7**, as a comparison analysis, it can be observed the average mechano-responsive voltage and current output peaks of the devices. The mechano-responsive outputs of the devices corroborate with the electrical performance and morphological analysis of the samples (section 3.2). RFP3 after functionalization showed great fibers distribution with a homogeneous formation of polyaniline along the walls of the pores, whereas sample RFP2 did not achieve full polymerization of the cellulose matrix and several holes between non-oriented fibers were observed (**figure 3.4**). When comparing the electrical performance of the samples (**table 3.4**), the resistance and mobility mirrored the performance of the devices in general.

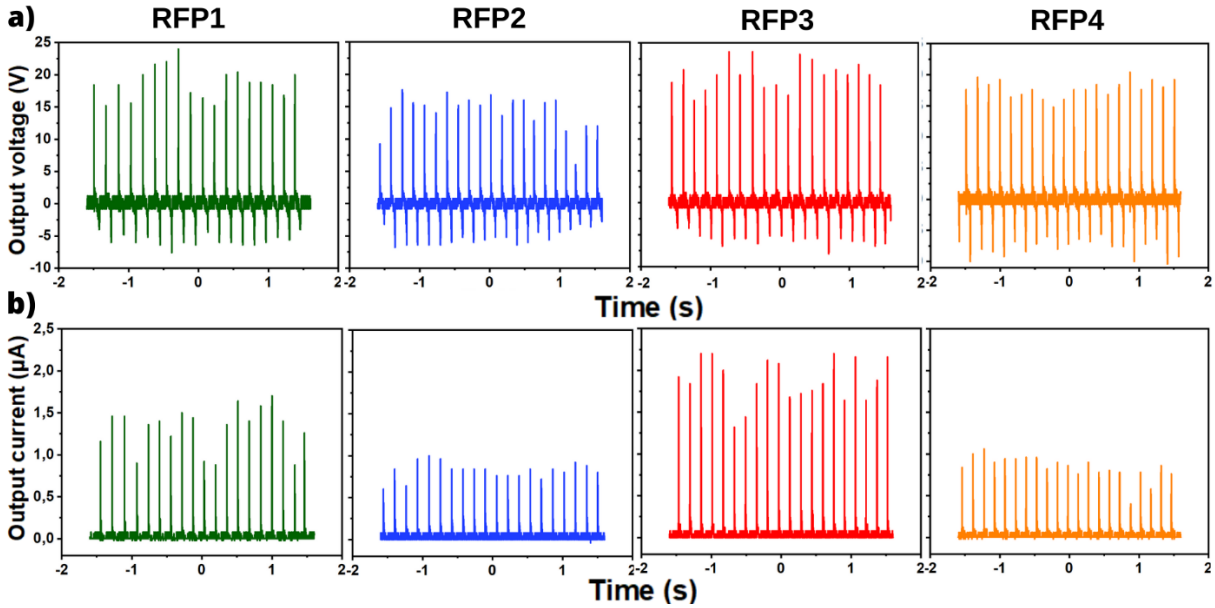


**Figure 3.7** - Plots of output mechano-responsive current and output voltage of all RFP devices. a) presents the average peaks of output voltage on an open circuit of all devices and b) presents the average output current on a short circuit of all devices.

Although values do not have a large discrepancy, it is observed the best performance on current and voltage output of the device with the highest fiber density (RFP3). It is also noticeable the non-constant peaks on most mechano-responsive transfers. This phenomenon is expectable due to the application of mechanical input with finger pressure, which can be influenced by different

factors, such as impact area and different sensitivity on specific areas of the devices since it is not an exact mechanism.

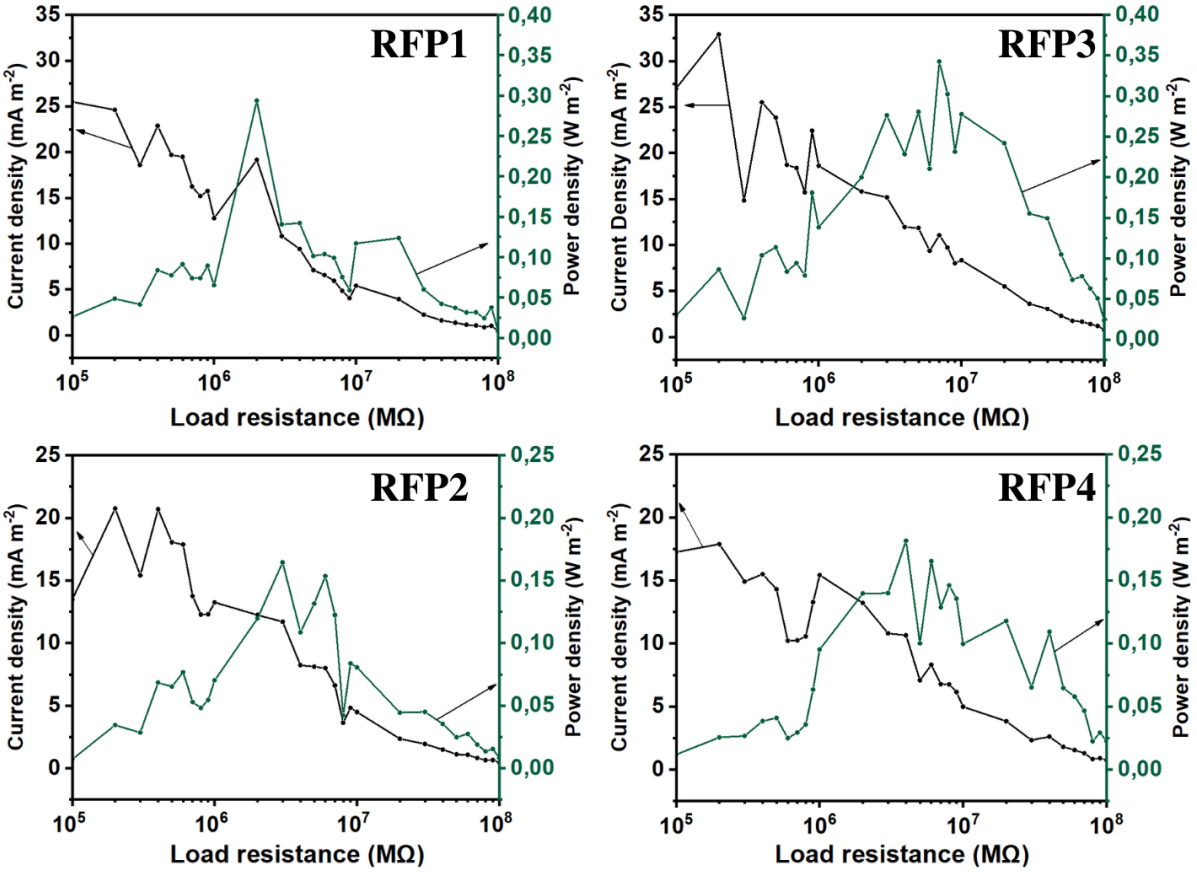


**Figure 3.8** - Current density and power density for different load resistances applied in series to the device. These results were achieved due to output voltage from mechano-responsive stimulus on each RFP energy devices.

To analyze the power and current density of the charge transfer on the devices, several load resistances, from 100 kΩ to 100 MΩ, were added in series on a rectifier circuit to evaluate the output performance of different external loads. The current density was calculated in function of the area of the cellulose samples (2x2 $cm^2$) and the output voltage on each resistance. As the electrical output of each resistance was measured, the power density of the devices was calculated. The curves of current and power density output of all devices can be observed on the double-y graphics, in **figure 3.8.**

When analyzing the electrical curves, it is noticed at first, the decrease of current density with the increase of load resistance, and a peak of power density between 0.16 and 0.35 W $m^{-2}$, between all devices.

The curves on power density correspond to the same performance of voltage and current output, leading to a device RFP2 with the lowest peak of power density (0.17 W $m^{-2}$) and device RFP3 with the maximum power density, $P_{max}$ (0.35 W $m^{-2}$). Also, device RFP3, achieved the

maximum power density, $I_{max}$ of 32.9 mA $m^{-2}$. Meanwhile, it is noticed a good performance from device RFP1, which had the most stable current density that reflects the same peak performance as the current density, with a combined peak at 2 MΩ.

### 3.4.2 Eco-Energy Devices applications

Due to the efficiency of harvesting electrical output with mechanical stimulus inputs of the eco-designed energy devices, it was approached a method of applying these electrical impulses on instant lighting with several blue LEDs. The mechanical inputs lightened several LEDs connected in series, since it was possible to generate high voltage output from the device to power up the LEDs. In **figure 3.9** it can be observed the LEDs connected in series produce instantaneous light from RFP3 and the schematic of the respective rectifier circuit. Alternatively, the LEDs were connected in parallel but since these are low-power devices there was no light production. It is necessary more current output to have an effective performance on instant light generation.

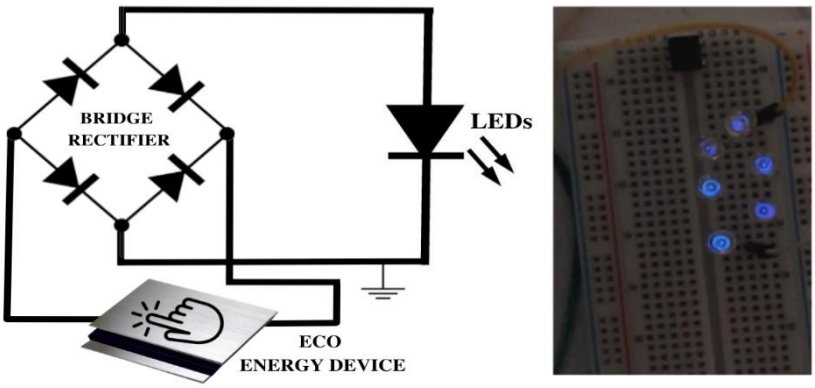


**Figure 3.9** - Photograph of device RFP3 electrical output performance on flash lighting 6 LEDs connected in series and respective schematic of the rectifier circuit.

## 3.5 Pressure Sensors

After the achievement the good electrical performances from mechano-stimulus eco-energy harvester using RFP as an active device layer, the next challenge was to produce a paper-based pressure sensor, with the functionalized samples.

Recently, the application of conductive paper-based materials is evolving at a fast pace in wearable electronics. With this ecological approach to energy science, several conventional materials are being substituted with new functional "green" materials with better mechanical and economic advantages [51], having a huge impact on socio-economic strategies.

Therefore, in this thesis, RFP samples were also explored as a pressure sensor application. The device was fabricated in a sandwich structure, where two electrode layers (screen-printed silver on paper) were coupled with the RFP samples as shown in **figure 3.10**. Because of the spongy structure of RFP samples, it makes a good opportunity to use it in resistive paper-based pressure sensor. Moreover, due to recyclability of used newspaper, it can be possible to replace the expensive and excess use of new raw materials that are used in previous pressure sensors investigations [52], [53]. Although these studies report great sensing performance, the limitation on their large-scale fabrication is a barrier due to expendable materials. Hence the production of the cellulose-based sensor is escalating due to their availability and conductive performance.

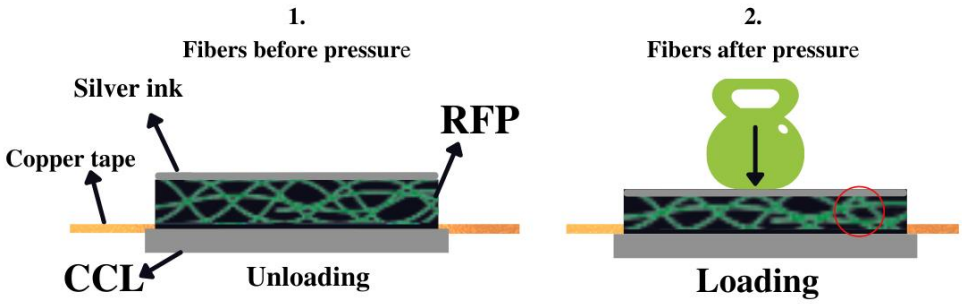


**Figure 3.10** - Schematic representation of the paper-based pressure sensors (unloading and loading mechanism).

The main objective of the pressure sensor electrical characterization is to observe the effect of voltage when applied different weights in different experiments. For the electrical characterization, it was used the same customized electronic circuit. An Arduino, which is a physical programmable circuit board performing as ground, as battery powering up the circuit with 5V, and as voltage meter on the sensor terminals (A0). On all measures, it was used a 100 kΩ load. The schematic of the electrical circuit and a snapshot of the pressure sensor electrical characterization are illustrated in **figure 3.11**.

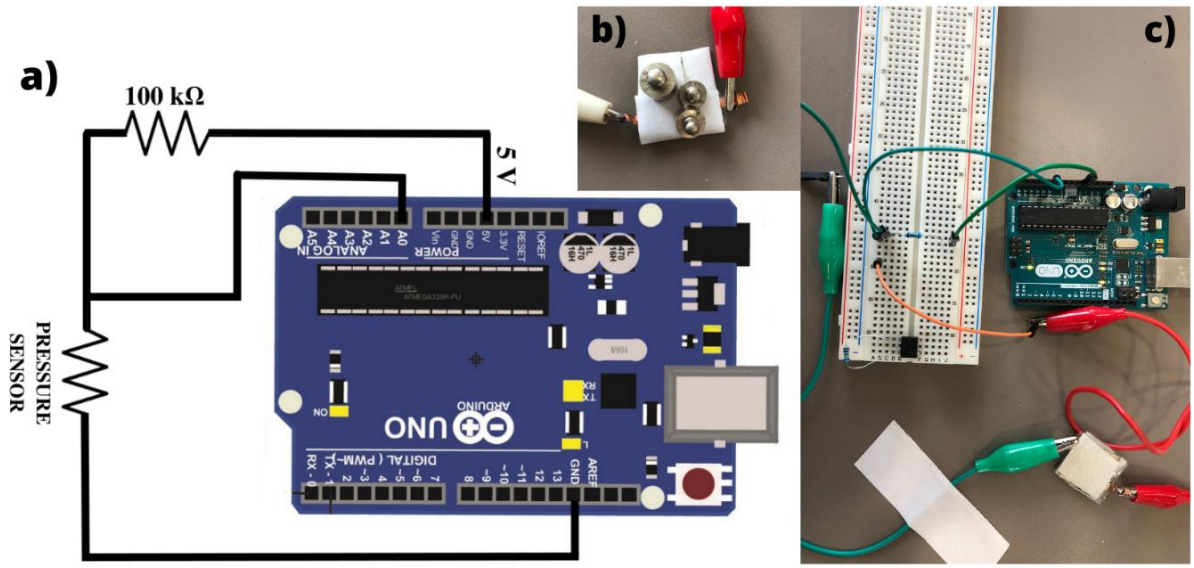


**Figure 3.11** - a) Pressure sensor circuit; b) Up-close photograph of the pressure sensor with 8g weights; c) photo of the pressure sensor overall output characterization with an Arduino board and a 100 kΩ load resistance.

The electrical performance of the pressure sensor was observed in two different phases. At first, it was measured the voltage output when applied to different pressure ranges of 5g to 25g weights for 140 seconds. With these measurements, it is intended to calculate the decrease of voltage instantly when the weight is applied on the sensor and the time of response of the pressure sensor to stabilize after this peak. In **figure 3.12a**, it is plotted the electrical performance of the resistive pressure sensor RFP3 when applied 5 load weights (5, 10, 20, 50, 100g) for 120 seconds approximately. Although the lowest weight had a bad performance, probably due to the sensitivity range of the layers, the other measures were very impressive with a peak of voltage decrease between 0.8 V and 1.2 V. The resistive sensor had a medium voltage of 5 V, which decreased to an average of 4.1 V (not with 5 g), with a fast stabilization in less than 40 seconds. This voltage decrease is directly proportional to a decrease in resistance ®, meaning the conductivity of the sensor will increase significantly. In all the measurement system the effective area of the device where the load was applied is 1 $cm^2$.

After, the same idea was processed in a lift/no lift method (**figure 3.12b)**, where the device showed a fast response with a wide working range of voltage on most of the weights. With a load of 5 g, it is observed a peak of voltage instantly when the weight was added. However, the stabilization of the voltage with the pressure was high, which is the same behavior as the weight in the plot depicted in **figure 3.12a**, which is caused by the sensitivity as mentioned above. The electrical characterization of the resistive sensor was only done on the device RFP3 due to efficiency purposes. The results on the other devices were inconclusive or lacked voltage outputs, therefore they were excluded.

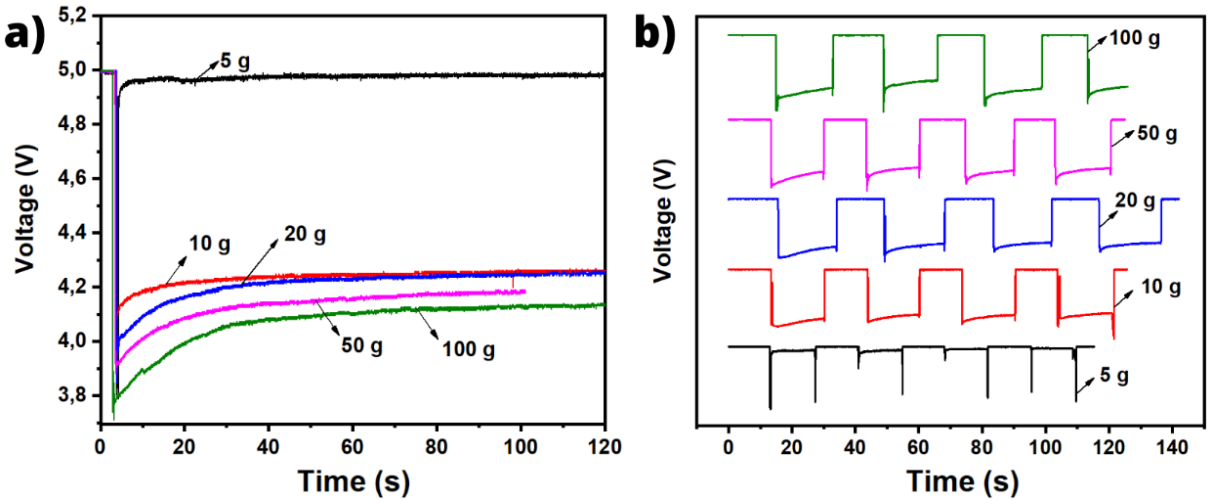


**Figure 3.12** - Electrical characterization of the pressure sensor: RFP3. a) Voltage monitored over time for five loading weights (measuring time: 120 seconds); b) Electrical performance of the device when submitted to several loading/unloading cycles. The protocol followed was: 15 seconds loaded, and 15 seconds recovery.

# 4 CONCLUSIONS AND FUTURE PERSPECTIVES

This work presents in several aspects a new approach of using recycled newspaper as an innovative concept of energy harvesting devices.

The paper, besides being a renewable material capable of recycling several times, and highly available, is mainly composed of cellulose fibers which have a splendid strength and absorbency, good electrical conductivity. Therefore, the recycling of black and white (BW) paper was made to fabricate cellulose samples, to be functionalized and applied to the production of energy devices and pressure sensors.

The first experimental part of this thesis was the recycling of newspapers, in the simplest possible way. Thus, after the separation of the color and the BW papers, a flotation technique to soften the paper and extract the most possible fillers and ink from them was used. Then, the recycled paper samples were obtained after filtration of the water and drying alternatively at room temperature and in an oven. As the recycled BW paper had better physical properties than the color one, it was used on all samples.

For the fabrication of the samples, it was established, after several trials, an average of 0.5 w/w% (0.83 g) to 165 ml of DI water. Several chemicals were used in different samples to tailor their morphology. In the overall, the chemical addiction did not lead to significant changes. However, the addition of NaCl to the samples, led to a variation of density and fibers distribution became more consistent (RP3).

Although cellulose is known for good conductivity, it is not capable of generating good electrical output without polymerization. Therefore, polyaniline (PANI), a well-known conjugated polymer, was synthesized with aniline and respective dopants and used to functionalize the paper.

Two methods were used: a two-step drop-casting and a suspension deep-casting. The first method was ineffective, due to the thickness and porosity of the samples, even if this method was more effective on filter paper or nanofibers. Nonetheless, the suspension method was effective, even with the high porosity of the samples, and the emeraldine (dark greenish-blue color) salt was achieved. Good conductivity was found on every sample, yet sample RFP3 was the most electrically efficient, with a sheet resistance ($R_{sh}$) of 670 $\Omega/cm^2$ and hall mobility ($\mu H$) of 163 $cm^2/V\text{-}s$.

Optical characterization was performed to analyze the chemical composition of samples before and after polymerization. The spectra have identified several bands that confirm the PANI formation among the fibers. Also, on Energy-Dispersion Spectroscopy (EDS), it was observed the

element mapping of the RFP, confirming the presence of sulphur and chlorine, which are elements that originated from the doping agents of the PANI.

Furthermore, the RFP samples were used as AL along with a silver metallic electrode printed on Whatman paper to build an ecological energy device, completely based on paper. The voltage and current output performance were satisfactory, for a recycled paper-based device. In general, the RFP3 was the device with better performance. This device achieved a maximum current and power density of 33 mA $m^{-2}$ and 0.35 W $m^{-2}$, respectively. The devices were used to light up LEDs directly with a charge transfer mechanism. When the RFP3 device was used, it was able to light up 6 blue LEDs in series. The same setup was not efficient when tried on 5 blue LEDs in a parallel circuit.

Finally, pressure sensors were fabricated with the same "zero e-waste" challenge as the energy devices, by generating a sensor completely based on paper. Using a metallic electrode printed on filter paper as an electrode layer and a PANI/cellulose recycled functionalized paper as an active layer. The electrical characterization was done to measure the sensor sensitivity against the variable pressure applied. When the pressure was applied on the sensor, with the different weights, a fast voltage decrease was measured, with an average of 1 V peaks, with a fast response and good stabilization.

The recycled paper achieved good physical properties, particularly when sodium chloride was added, which increased the density, improving the strength and uniformity of the cellulose fibers, exhibiting great flexibility and sponginess. Overall, the recycling of the newspaper into electronic applications was accomplished.

With the good results on energy harvesting and lighting applications, future research will be needed with a special focus on the charge-discharge with energy storage using paper-based supercapacitors. The effectiveness of these ecological hybrid paper-based energy devices captured interest due to their low-cost, accessibility, and mechanical advantages [54], [55].

The application of cellulose as the main substrate will improve the flexibility and lightness of the supercapacitor and reveal simultaneously a high electrical conductivity. A previous report [56] justifies the selection of PANI as the main conducting polymer, due to its simplistic electropolymerization. Since many supercapacitors are paper-based, the polyaniline, owing to their charging/discharging capability on a conducting state, will provide a conductive bridge between substrate and electrode and vice-versa. Nonetheless, the empowering of these mechanisms is making a massive change in sustainable energy storage, which can be fully adapted to future work for the eco-design supercapacitors, with the same methodology of the energy devices and pressure sensors.

In future work, some improvements can be made to paper technology to maximize the performance of the devices. These can include the introduction of sodium chloride on all samples, the

usage of sodium chlorite ($NaClO_2$) for bleaching techniques of the cellulose without losing any physical properties, and the replacement of the PANI with other conjugated polymers such as polypyrrole (PPy) [57], which can improve the paper conductivity leading to better electrical performance on paper-based energy devices.

# REFERENCES


[1] S. Herat, "Sustainable management of electronic waste (e-waste)," *Clean - Soil, Air, Water*, vol. 35, no. 4. pp. 305–310, Sep. 2007. doi: 10.1002/clen.200700022.

[2] e-waste on developing countries: https://www.borgenmagazine.com/global-e-waste-developing-countries/

[3] Global e-waste market: http://www.ipsnews.net/2020/07/global-e-waste-surging-21-5-years/

[4] Global e-waste hierarchy: https://www.theatlantic.com/technology/archive/2016/09/the-global-cost-of-electronic-waste/502019/

[5] e-waste and the hazardous substances generated, https://tcocertified.com/hazardous-substances/

[6] A. P. M. Velenturf and P. Purnell, "Principles for a sustainable circular economy," *Sustainable Production and Consumption*, vol. 27. Elsevier B.V., pp. 1437–1457, Jul. 01, 2021. doi: 10.1016/j.spc.2021.02.018.

[7] Waste management on a circular economy approach, https://www.eea.europa.eu/publications/reducing-loss-of-resources-from

[8] J. Pluskal, R. Šomplák, V. Nevrlý, V. Smejkalová, and M. Pavlas, "Strategic decisions leading to sustainable waste management: Separation, sorting and recycling possibilities," *Journal of Cleaner Production*, vol. 278, Jan. 2021, doi: 10.1016/j.jclepro.2020.123359.

[9] H. Koga, H. Tonomura, M. Nogi, K. Suganuma, and Y. Nishina, "Fast, scalable, and eco-friendly fabrication of an energy storage paper electrode," in *Green Chemistry*, 2016, vol. 18, no. 4, pp. 1117–1124. doi: 10.1039/c5gc01949d.

[10] M. Hietala, K. Varrio, L. Berglund, J. Soini, and K. Oksman, "Potential of municipal solid waste paper as raw material for production of cellulose nanofibres," *Waste Management*, vol. 80, pp. 319–326, Oct. 2018, doi: 10.1016/j.wasman.2018.09.033.

[11] K. Sharma, K. Pareek, R. Rohan, and P. Kumar, "Flexible supercapacitor based on three-dimensional cellulose/graphite/polyaniline composite," *International Journal of Energy Research*, vol. 43, no. 1, pp. 604–611, Jan. 2019, doi: 10.1002/er.4277.

[12] R. Martins *et al.*, "Papertronics: Multigate paper transistor for multifunction applications," *Applied Materials Today*, vol. 12, pp. 402–414, Sep. 2018, doi: 10.1016/j.apmt.2018.07.002.

[13] H. Mianehrow, S. Sabury, A. M. Bazargan, F. Sharif, and S. Mazinani, "A flexible electrode based on recycled paper pulp and reduced graphene oxide composite," *Journal of*

*Materials Science: Materials in Electronics*, vol. 28, no. 6, pp. 4990–4996, Mar. 2017, doi: 10.1007/s10854-016-6153-2.

[14] A. M. Youssef, S. Kamel, M. El-Sakhawy, and M. A. el Samahy, "Structural and electrical properties of paper-polyaniline composite," *Carbohydrate Polymers*, vol. 90, no. 2, pp. 1003–1007, Oct. 2012, doi: 10.1016/j.carbpol.2012.06.034.

[15] G. Ferreira, S. Goswami, S. Nandy, L. Pereira, R. Martins, and E. Fortunato, "Touch-Interactive Flexible Sustainable Energy Harvester and Self-Powered Smart Card," *Advanced Functional Materials*, vol. 30, no. 5, Jan. 2020, doi: 10.1002/adfm.201908994.

[16] D. Kannichankandy *et al.*, "Flexible piezo-resistive pressure sensor based on conducting PANI on paper substrate," *Synthetic Metals*, vol. 273, Mar. 2021, doi: 10.1016/j.synthmet.2021.116697.

[17] J. Yu *et al.*, "Flexible metallic fabric supercapacitor based on graphene/polyaniline composites," *Electrochimica Acta*, vol. 259, pp. 968–974, Jan. 2018, doi: 10.1016/j.electacta.2017.11.008.

[18] Y. Zhao, S. Si, and C. Liao, "A single flow zinc//polyaniline suspension rechargeable battery," *Journal of Power Sources*, vol. 241, pp. 449–453, 2013, doi: 10.1016/j.jpowsour.2013.04.095.

[19] J. R. Posdorfer, B. Werner, B. Wessling, S. Heun, and H. Becker, "Influence of conductivity and work function of polyaniline-based HIL on PLED device performance," in *Organic Light-Emitting Materials and Devices VII*, Feb. 2004, vol. 5214, p. 188. doi: 10.1117/12.510006.

[20] S. K. Dhawan, D. Kumar, M. K. Ram, S. Chandra, and D. C. Trivedi, "ACTW1)RS B CHEMICAL Application of conducting polyaniline as sensor material for ammonia," 1997, pp. 99-103. doi: 0925-4005/97/S17.00

[21] Z. M. Tahir, E. C. Alocilja, and D. L. Grooms, "Polyaniline synthesis and its biosensor application," in *Biosensors and Bioelectronics*, Feb. 2005, vol. 20, no. 8 SPEC. ISS., pp. 1690–1695. doi: 10.1016/j.bios.2004.08.008.

[22] G. Wang, R. Vivek, and J.-Y. Wang, "Mini-Reviews in Organic Chemistry SCIENCE BENTHAM Impact Factor: 1.394,"; 2017,ISSN:1875-6298,doi: 10.2174/1570193X14666161118114.

[23] S. Goswami *et al.*, "Human-motion interactive energy harvester based on polyaniline functionalized textile fibers following metal/polymer mechano-responsive charge transfer mechanism," *Nano Energy*, vol. 60, pp. 794–801, Jun. 2019, doi: 10.1016/j.nanoen.2019.04.012.

[24] Statistics of generation of greenhouse gas emissions via electricity production: https://www.epa.gov/ghgemissions/sources-greenhouse-gas-emissions#electricity

[25] W. Wang, V. Cionca, N. Wang, M. Hayes, B. O'Flynn, and C. O'Mathuna, "Thermoelectric energy harvesting for building energy management wireless sensor networks," *International Journal of Distributed Sensor Networks*, vol. 2013, 2013, doi: 10.1155/2013/232438.

[26] C. Wu, T. W. Kima, S. Sung, J. H. Park, and F. Li, "Ultrasoft and cuttable paper-based triboelectric nanogenerators for mechanical energy harvesting," *Nano Energy*, vol. 44, pp. 279–287, Feb. 2018, doi: 10.1016/j.nanoen.2017.11.080.

[27] V. Annapureddy *et al.*, "Exceeding milli-watt powering magneto-mechano-electric generator for standalone-powered electronics," *Energy and Environmental Science*, vol. 11, no. 4, pp. 818–829, Apr. 2018, doi: 10.1039/c7ee03429f.

[28] S. Chen, J. Jiang, F. Xu, and S. Gong, "Crepe cellulose paper and nitrocellulose membrane-based triboelectric nanogenerators for energy harvesting and self-powered human-machine interaction," *Nano Energy*, vol. 61, pp. 69–77, Jul. 2019, doi: 10.1016/j.nanoen.2019.04.043.

[29] M. Uno and K. Tanaka, "Accelerated charge-discharge cycling test and cycle life prediction model for supercapacitors in alternative battery applications," *IEEE Transactions on Industrial Electronics*, vol. 59, no. 12, pp. 4704–4712, 2012, doi: 10.1109/TIE.2011.2182018.

[30] L. Q. Tao *et al.*, "Graphene-Paper Pressure Sensor for Detecting Human Motions," *ACS Nano*, vol. 11, no. 9, pp. 8790–8795, Sep. 2017, doi: 10.1021/acsnano.7b02826.

[31] L. Gao *et al.*, "All Paper-Based Flexible and Wearable Piezoresistive Pressure Sensor," *ACS Applied Materials and Interfaces*, vol. 11, no. 28, pp. 25034–25042, Jun. 2019, doi: 10.1021/acsami.9b07465.

[32] H. Yu, H. Han, J. Jang, and S. Cho, "Fabrication and Optimization of Conductive Paper Based on Screen-Printed Polyaniline/Graphene Patterns for Nerve Agent Detection," *ACS Omega*, vol. 4, no. 3, pp. 5586–5594, Mar. 2019, doi: 10.1021/acsomega.9b00371.

[33] K. Liu *et al.*, "Polyaniline nanofiber wrapped fabric for high performance flexible pressure sensors," *Polymers*, vol. 11, no. 7, 2019, doi: 10.3390/polym11071120.

[34] A. Iosip, R. Nicu, F. Ciolacu, and E. Bobu, "INFLUENCE OF RECOVERED PAPER QUALITY ON RECYCLED PULP PROPERTIES," 2010, pp. 513-519. 44 (10(.

[35] N. Wistara and R. A. Young, "Properties and treatments of pulps from recycled paper. Part I. Physical and chemical properties of pulps," 1999; pp. 291-329.

[36] N. Wistara, X. Zhang, and R. A. Young, "Properties and treatments of pulps from recycled paper. Part II. Surface properties and crystallinity of fibers and fines," 1999. Pp. 325-48

[37] M. G. A. Vieira and S. C. S. Rocha, “Drying conditions influence on physical properties of recycled paper,” *Chemical Engineering and Processing: Process Intensification*, vol. 46, no. 10, pp. 955–963, Oct. 2007, doi: 10.1016/j.cep.2007.06.006.

[38] P. Widsten, N. Dooley, R. Parr, J. Capricho, and I. Suckling, “Citric acid crosslinking of paper products for improved high-humidity performance,” *Carbohydrate Polymers*, vol. 101, no. 1, pp. 998–1004, 2014, doi: 10.1016/j.carbpol.2013.10.002.

[39] A. Ottenhall, T. Seppänen, and M. Ek, “Water-stable cellulose fiber foam with antimicrobial properties for bio based low-density materials,” *Cellulose*, vol. 25, no. 4, pp. 2599–2613, Apr. 2018, doi: 10.1007/s10570-018-1738-y.

[40] M. v. Kulkarni and A. K. Viswanath, “Scanning electron microscopy, spectroscopy, and thermal studies of polyaniline doped with various sulfonic acids,” *Journal of Macromolecular Science - Pure and Applied Chemistry*, vol. 41 A, no. 10, pp. 1173–1186, Sep. 2004, doi: 10.1081/MA-200026566.

[41] K. Daideche, L. Hasniou, and D. Lerari, “Electro Synthesis and Characterization of PANI and PANI/ZnO Composites Films,” *Chemistry Proceedings*, vol. 3, no. 1, p. 110, Nov. 2020, doi: 10.3390/ecsoc-24-08328.

[42] V. Hospodarova, E. Singovszka, and N. Stevulova, “Characterization of Cellulosic Fibers by FTIR Spectroscopy for Their Further Implementation to Building Materials,” *American Journal of Analytical Chemistry*, vol. 09, no. 06, pp. 303–310, 2018, doi: 10.4236/ajac.2018.96023.

[43] W. H. Danial, Z. Abdul Majid, M. N. Mohd Muhid, M. B. Bakar, Z. Ramli, and S. Triwahyono, “Preparation of Cellulose Nanocrystal Aerogel from Wastepaper through Freeze-Drying Technique,” *Advanced Materials Research*, vol. 1125, pp. 296–300, Oct. 2015, doi: 10.4028/www.scientific.net/amr.1125.296.

[44] S. Goswami, M. K. Mitra, and K. K. Chattopadhyay, “Enhanced field emission from polyaniline nano-porous thin films on PET substrate,” *Synthetic Metals*, vol. 159, no. 23–24, pp. 2430–2436, Dec. 2009, doi: 10.1016/j.synthmet.2009.08.007.

[45] T. Rajyalakshmi, A. Pasha, S. Khasim, M. Lakshmi, and M. Imran, “Synthesis, characterization and Hall-effect studies of highly conductive polyaniline/graphene nanocomposites,” *SN Applied Sciences*, vol. 2, no. 4, Apr. 2020, doi: 10.1007/s42452-020-2349-4.

[46] D. S. Dhawale, R. R. Salunkhe, V. S. Jamadade, D. P. Dubal, S. M. Pawar, and C. D. Lokhande, “Hydrophilic polyaniline nanofibrous architecture using electrosynthesis method for supercapacitor application,” *Current Applied Physics*, vol. 10, no. 3, pp. 904–909, May 2010, doi: 10.1016/j.cap.2009.10.020.

[47] P. P. Sengupta, P. Kar, and B. Adhikari, “Effect of LiCl as an additive in the polymerization reaction of aniline and its influence on the structural and electrical property of polyaniline,” *Reactive and Functional Polymers*, vol. 68, no. 6, pp. 1103–1112, Jun. 2008, doi: 10.1016/j.reactfunctpolym.2008.02.013.

[48] M. Mitra *et al.*, “Reduced graphene oxide-polyaniline composites - Synthesis, characterization and optimization for thermoelectric applications,” *RSC Advances*, vol. 5, no. 39, pp. 31039–31048, 2015, doi: 10.1039/c5ra01794g.

[49] H. Wang, S. I. Yi, X. Pu, and C. Yu, “Simultaneously improving electrical conductivity and thermopower of polyaniline composites by utilizing carbon nanotubes as high mobility conduits,” *ACS Applied Materials and Interfaces*, vol. 7, no. 18, pp. 9589–9597, May 2015, doi: 10.1021/acsami.5b01149.

[50] J. Cho *et al.*, “High Charge-Carrier Mobility of 2.5 cm2 V-1 s-1 from a Water-Borne Colloid of a Polymeric Semiconductor via Smart Surfactant Engineering,” *Advanced Materials*, vol. 27, no. 37, pp. 5587–5592, Oct. 2015, doi: 10.1002/adma.201503122.

[51] S. Chen, Y. Song, and F. Xu, “Flexible and Highly Sensitive Resistive Pressure Sensor Based on Carbonized Crepe Paper with Corrugated Structure,” *ACS Applied Materials and Interfaces*, vol. 10, no. 40, pp. 34646–34654, Oct. 2018, doi: 10.1021/acsami.8b13535.

[52] Y. Guo, Z. Guo, M. Zhong, P. Wan, W. Zhang, and L. Zhang, “A Flexible Wearable Pressure Sensor with Bioinspired Microcrack and Interlocking for Full-Range Human–Machine Interfacing,” *Small*, vol. 14, no. 44, Nov. 2018, doi: 10.1002/smll.201803018.

[53] X. P. Li *et al.*, “Highly sensitive, reliable and flexible piezoresistive pressure sensors featuring polyurethane sponge coated with MXene sheets,” *Journal of Colloid and Interface Science*, vol. 542, pp. 54–62, Apr. 2019, doi: 10.1016/j.jcis.2019.01.123.

[54] S. Alipoori, S. Mazinani, S. H. Aboutalebi, and F. Sharif, “Review of PVA-based gel polymer electrolytes in flexible solid-state supercapacitors: Opportunities and challenges,” *Journal of Energy Storage*, vol. 27. Elsevier Ltd, Feb. 01, 2020. doi: 10.1016/j.est.2019.101072.

[55] L. Yuan *et al.*, “Paper-based supercapacitors for self-powered nanosystems,” *Angewandte Chemie - International Edition*, vol. 51, no. 20, pp. 4934–4938, May 2012, doi: 10.1002/anie.201109142.

[56] A. Eftekhari, L. Li, and Y. Yang, “Polyaniline supercapacitors,” *Journal of Power Sources*, vol. 347. Elsevier B.V., pp. 86–107, 2017. doi: 10.1016/j.jpowsour.2017.02.054.

[57] L. Yuan, B. Yao, B. Hu, K. Huo, W. Chen, and J. Zhou, “Polypyrrole-coated paper for flexible solid-state energy storage,” *Energy and Environmental Science*, vol. 6, no. 2, pp. 470–476, 2013, doi: 10.1039/c2ee23977a.

# ANNEXES

## Annex A - Materials and methods

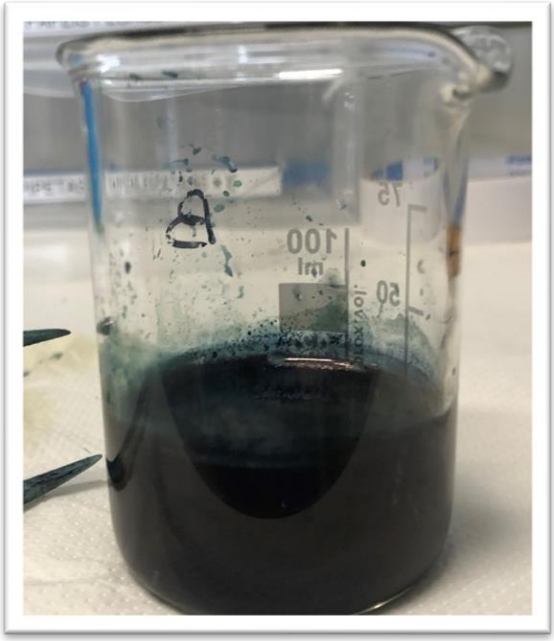

**Figure A.3** - Polyaniline synthesis for the deep-casting functionalization, the dark greenish-blue color confirms the emeraldine salt oxidation.

**Figure A.4** - Photograph of the silver ink electrode used as charge collector on the energy devices.

# Annex B – Results and discussion

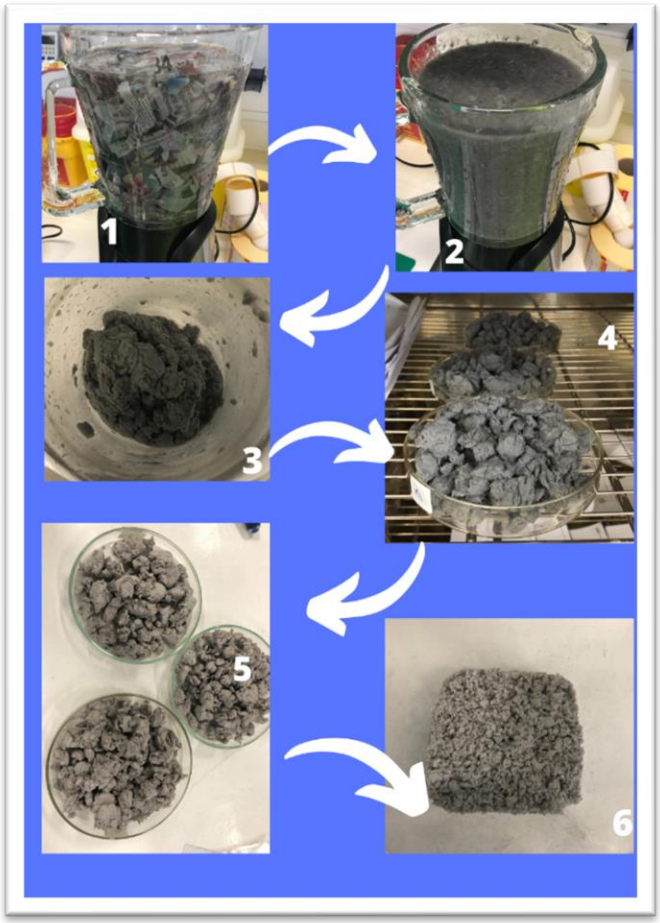


**Figure B.1** – Step-by-step photographs of the newspaper recycling process.

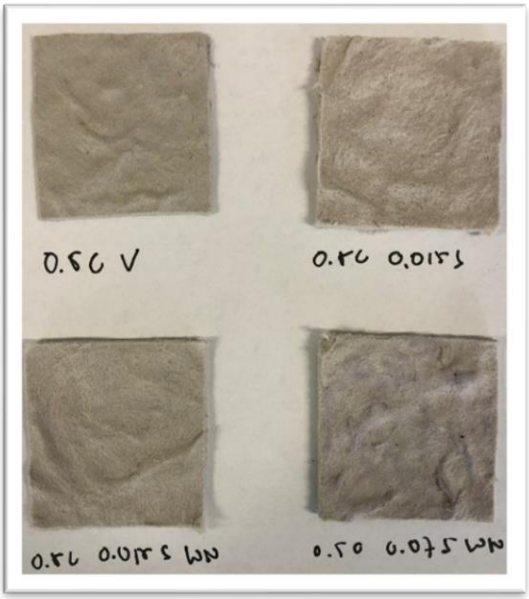

**Figure B.2 -** Final recycled paper (RP) samples before functionalization.

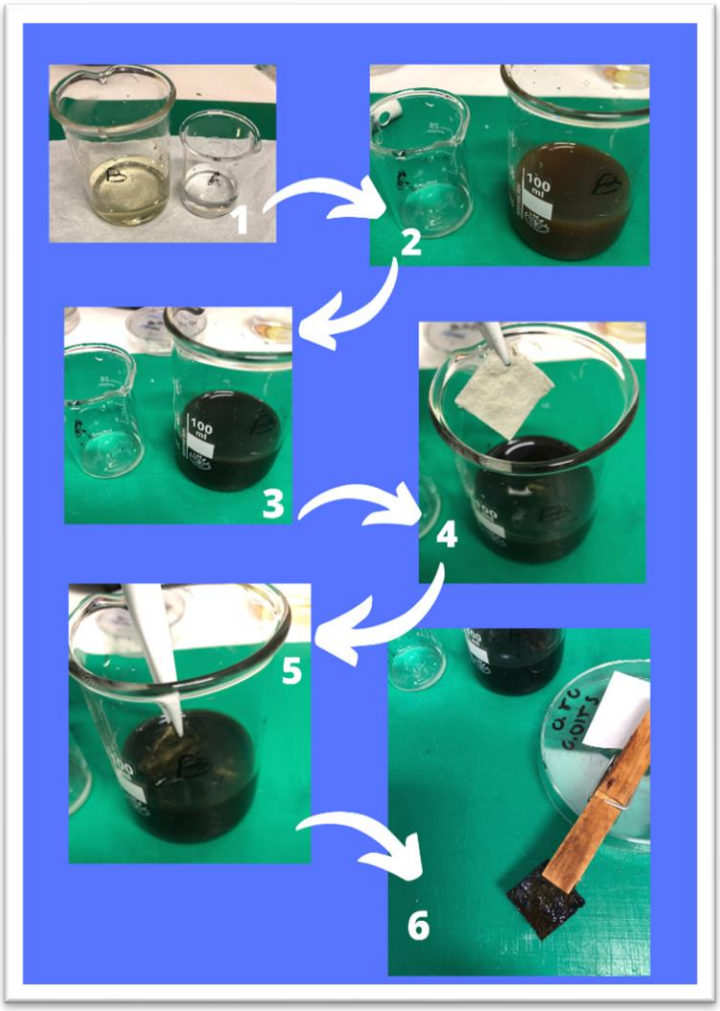


**Figure B.3 -** Step-by-step photographs of the deep-cast method (suspension) of RP**.**

**Figure B.4 -** Sample functionalized with two-step drop-casting method (left) and sample functionalized with suspension/deep-casting method (right). Emeraldine state was achieved on the suspension method (dark greenish-blue) and not achieved on the drop-casting method (greenish-yellow).

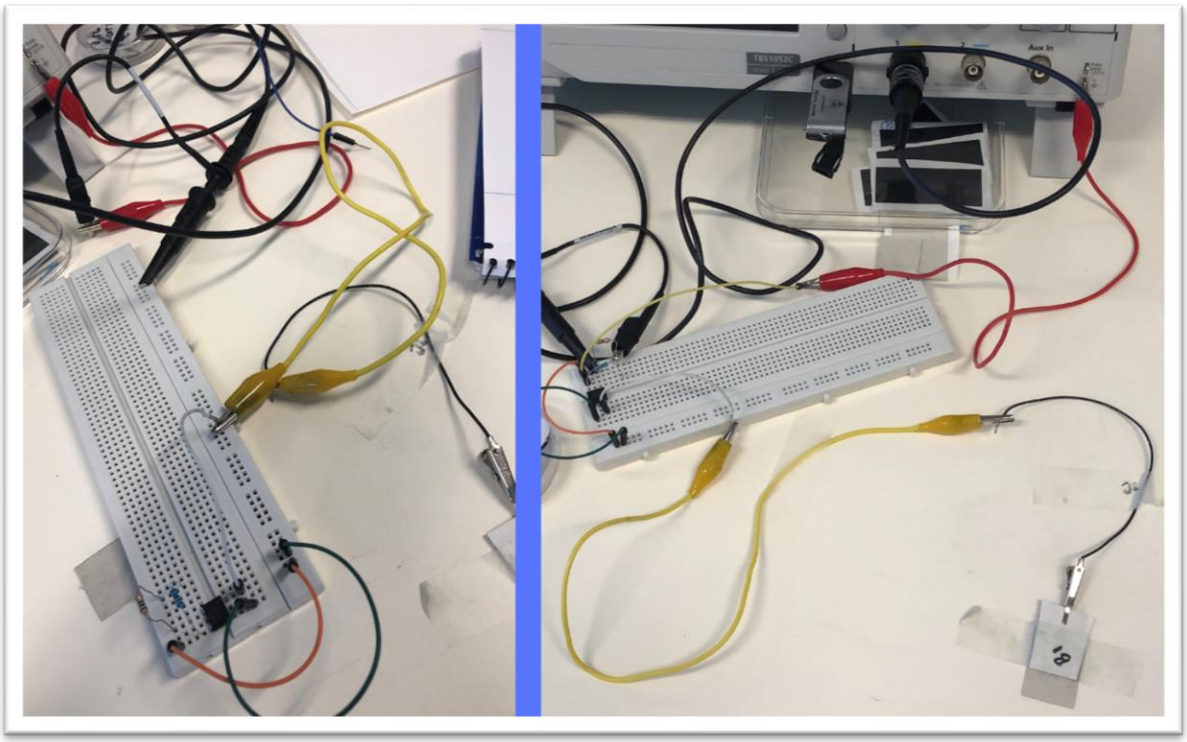

**Figure B.5** – Open circuit ($V_{oc}$) and short circuit ($I_{sc}$) rectifier, respectively.